Standard Operating Procedure (SOP)
Constructing YJACK Q-s Plot from YJACK BD Pile Load Test
YPLOT 2020.0101

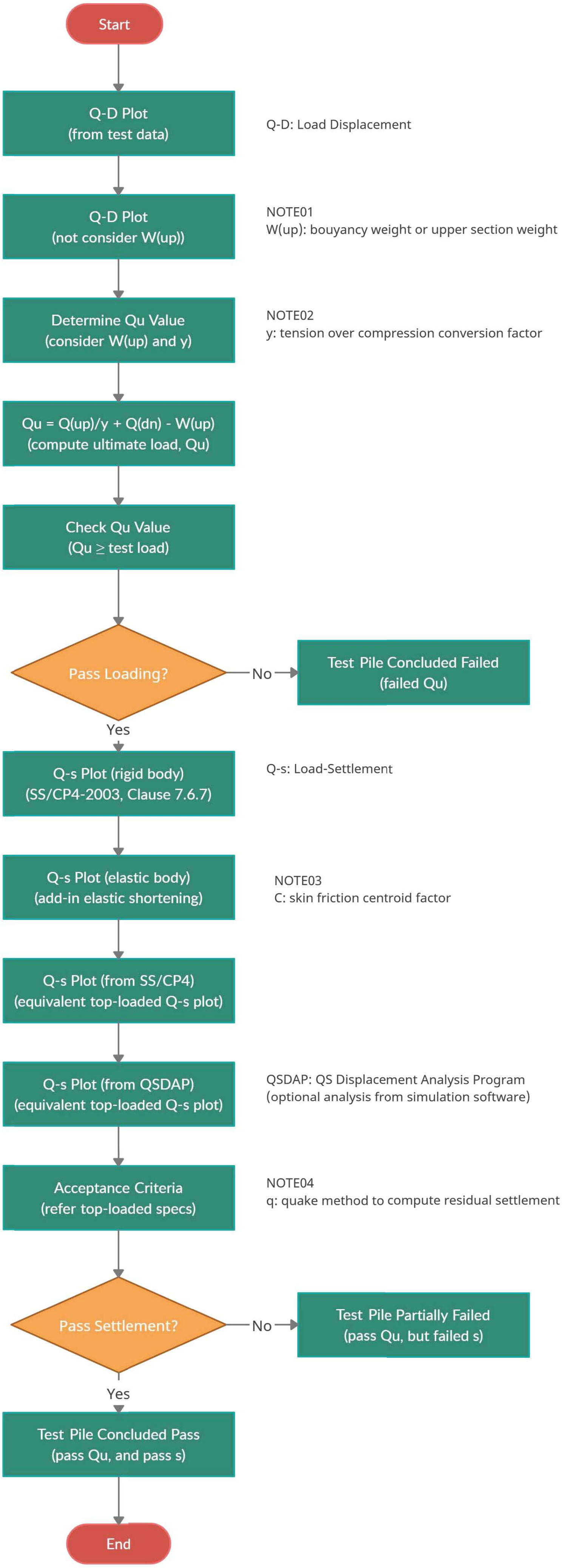

YPLOT
13
Analysis

YPLOT, NOTE01

W(up): Buoyancy Weight or Upper Section Weight

Buoyant weight or pile upper section weight, W(up), is a constant value. It is relatively small compared to test load, Q.

In long pile condition, the early loading step (i), the test load, Q(i), may low value, but after considerations to subtract the measured Q(i) value with W(up), the load~displacement, Q~D, data points may have negative values to indicate "negative friction", in which this does not make sense. Hence in YJACK Plot Method (named as YPLOT), W(up) will be ignored in plotting the Q~D Plot.

Subsequently to consider this W(up) in-conjunction with tension over compression conversion factor, γ, to evaluate ultimate load, Qu value using following equation:

$$Qu = Q(up)/\gamma + Q(dn) - W(up)$$

in which:

Qu	: ultimate load
Q(up)	: upper section load measured from bi-directional pile load test
Q(dn)	: lower section load measured from bi-directional pile load test
W(up)	: upper section weight (= buoyancy weight)
γ	: tension over compression conversion factor

Reference A:

Tech Paper Proceeding 3rd International Conference in Geotechnical Engineering, 1993

(Uplift Capacity of Driven Piles from Static Load Tests)

Document NOTE01, Reference A

Tech Paper Proceeding 3rd International Conference in Geotechnical Engineering, 1993

(Uplift Capacity of Driven Piles from Static Load Tests)

Proceedings: Third International Conference on Case Histories in Geotechnical Engineering, St. Louis, Missouri, June 1-4, 1993, Paper No. 1.02

Uplift Capacity of Driven Piles From Static Loading Tests

M. H. Hussein
Partner, Goble Rausche Likins and Associates, Inc., Orlando, Florida

J. M. Sheahan
Senior Geotechnical Engineer, HDR Engineering Inc., Pittsburgh, Pennsylvania

Synopsis: A pile driving and testing program was undertaken to evaluate installation procedures, assess capacity (particularly in uplift) of 24- and 30-inch square, prestressed concrete piles, and provide foundation design parameters for the New Edison Bridge project in Fort Myers, Florida. The subsurface profile generally consisted of three major soil strata: an upper clayey sand and sandy clay layer to a depth of about 45 to 50 feet below mudline, a medium dense to dense silty sand middle layer about 10 feet thick, and a third layer of dense to very dense silty fine sand. Eleven prestressed concrete test piles of varying length were driven at five test sites and uplift tests were performed to allow an independent evaluation of the different soil layers. All piles were dynamically monitored during installation and restrikes to evaluate pile drivability and bearing capacity including time related capacity increases due to soil "set-up." This paper presents descriptions of the pile driving and load testing program along with findings regarding pile uplift capacities from load tests, pile capacities from dynamic testing, soil-pile adhesion values, wave equation factors, soil strength vs time dependency, foundation design and pile driving recommendations.

1. INTRODUCTION

The existing 60 year old, two-lane draw-bridge structure (known as the Edison Bridge) carries Route 41 over the Caloosahatchee River in Fort Myers, Florida and will be replaced by two separate bridges, each approximately one mile in length, for north- and south-bound traffic. The main spans will be 56 feet high to accommodate boat traffic through the relocated river channel. The project cost is estimated at 40 million dollars.

Structural, geotechnical, design ship-impact loading and other considerations required that the new bridges be founded on high-capacity driven piles. Subsurface investigations, geotechnical studies, and a pile load test program were undertaken as part of the foundation design process. A benefit/cost analysis indicated that a load test program was justified to determine pile ultimate uplift capacities and to examine pile drivability. Uplift capacity was an important consideration because of the need to design for ship impact loads on the substructure. Prestressed concrete 24- and 30-inch square piles were driven to varying penetrations at five test sites and uplift load tests were performed to allow an independent evaluation of each of the three major soil layers. Dynamic pile testing was performed during initial installation and restrikes to evaluate hammer performance, pile driving stresses and structural integrity, pile static bearing capacity and time related capacity increases due to soil set-up. This paper presents descriptions of the geotechnical investigations and pile driving and load testing procedures and results. Since the original work was performed using the English units system, the same will be used here. A conversion table to SI units is appended at the end of the paper.

2. GEOTECHNICAL INVESTIGATIONS

Test borings were taken at intervals of about 200 feet along the proposed bridge alignments and at each of the five pile test site locations. The water depth across the river ranged between 4 to 10 feet. Geotechnical investigations included Standard Penetration Testing (SPT) and laboratory analyses, and to a lesser extent Cone Penetration Testing (CPT) and Vane Shear Testing. Interpretation of borings defined four soil layers from mudline to below expected pile toe elevations. The upper most strata contained interbedded layers of fine sand with silt and organic fines and shell fragments, calcareous silty sand, and silty to clayey fine sand. The thickness of this layer varies between 15 and 37 feet with N-values typically less than 10 blows per foot. Ocassionally, a medium dense layer was encountered. The estimated unit weight was 115 pounds per cubic foot (pcf) with no cohesion, and an average angle of internal friction of 27 degrees. The second layer had a thickness of 10 to 30 feet and consisted of sandy, medium to stiff clay with lenses of calcareous clayey fine sand and shell traces. This layer had N-values between 0 and 30 although most were typically below 10, and a unit weight of 115 pcf. Field vane shear tests in this interval showed an average undisturbed shear strength of about 3.10 ksf and an average disturbed shear strength of 1.34 ksf. Unconsolidated, undrained triaxial tests showed an average shear strength of 1.24 ksf with no angle of internal friction. These two upper layers together were typically about 45 to 50 feet thick. The third layer was 5 to 15 ft thick and contained medium dense to dense silty sand with shell and gravel size limestone and cemented sand fragments. It had an estimated unit weight of 125 pcf, no cohesion and an average internal friction angle of 35 degrees based on N-values between 15 and 30. The bottom layer was a dense to very dense silty fine sand with N-values ranging from 30 to more than 100. Most were greater than 50 per foot. The estimated soil parameters for this layer were a unit weight of 125 pcf, an angle of internal friction of 40 degrees, and no cohesion. For the purposes of analyzing the test pile data, layers 1 and 2 were combined. Therefore, subsequent reference to the soil layers will be to Layers I, II, and III as illustrated in the idealized profile presented in Figure 1.

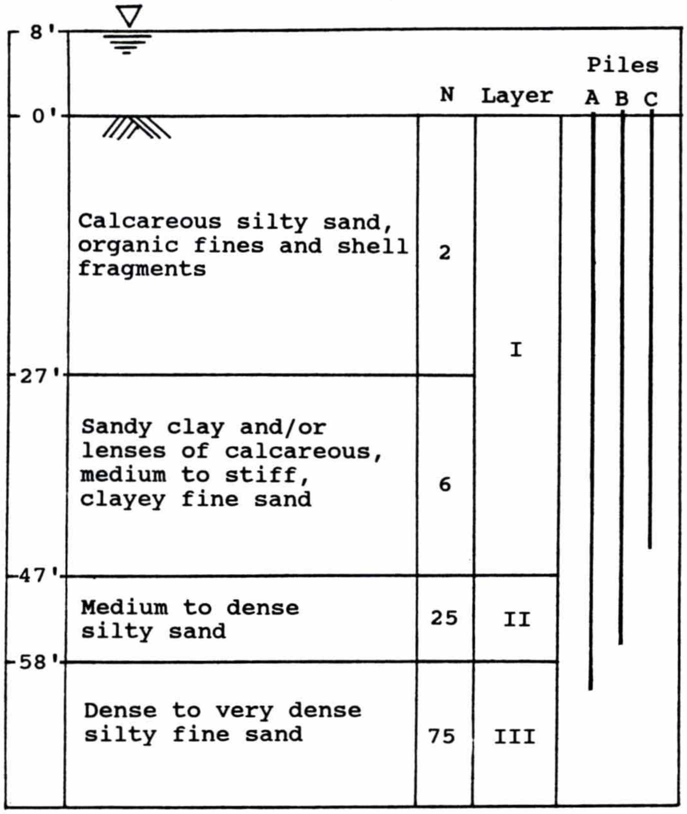

FIGURE 1 Idealized general soil profile

3. PILE INSTALLATION

Five test site locations (Sites 1 through 5) that represent subsurface conditions along the project length were chosen. A total of 11 test piles were driven. Piles whose tips were stopped in soil layers I, II, and III are referred to as C, B, and A piles, respectively as illustrated in Figure 1. Sites 1 and 5 each had one 30-inch square, A-type pile. Sites 2 and 3 each had three 24-inch square piles, one each of the A-, B- and C-type. Site 4 had three 30-inch square piles, one of each type. Piles are distinguished by their site number and pile type (e.g., 1A, 2C, etc.). All piles were initially driven during the first week of November, and some were restruck several times after intervals of up to 13 days thereafter.

The prestressed concrete test piles were cast between October 13 and 24th. The 30-inch piles had 28, 1/2 inch steel strands each tensioned with 28.1 kips and the 24-inch piles had 24, 1/2 inch strands prestressed to 29 kips each, both pile sizes had the same No. 5 gauge spiral ties. Concrete design strength was 6 ksi at 28 days. Sample concrete cylinders made from each pile at the time of casting were tested on the days of pile driving and static load testing. At the day of driving, two to three weeks after casting, concrete strengths were between 6.1 and 7.6 ksi, and the elastic moduli were between 3900 and 4400 ksi. Telltale casings were cast into the piles with the intention of determining load distribution and soil adhesion from static load tests.

Pile driving and restriking were accomplished with a Conmaco 5300-E5 single acting air hammer. The particular hammer used had a ram weight of 30 kips and was fitted with a cam rod allowing it to operate at 2 and 4 ft strokes, corresponding to rated energies of 60 and 120 kip-ft, respectively. The hammer cushion was six inches of blue polymer and was "cooled" during pile driving with water injected into the upper side of the pile cap. The effect of introducing this "cooling" water on energy transfer will be discussed. New sheets of plywood with total initial thickness of 6.75 inches and the same size as the pile were used in each case. Pile cap weights were 6.1 and 7.0 kips for the 24- and 30-inch piles, respectively. In some cases, the entire pile installation was accomplished with a 2-foot hammer stroke, while in others, the stroke was changed to 4-foot when driving became relatively hard. Table 1 lists the end of driving hammer stroke and driving resistance in blows per foot (BPF) for each pile. This table also includes results from dynamic testing which will be discussed further.

At each site the A-type piles were driven first into Layer III to obtain the project target compressive capacity and examine pile drivability. Piles of the B- and C-type were then driven in that order to a specific elevation based on the driving record of the A pile and boring information at the site.

4. DYNAMIC TESTING AND ANALYSES

Preliminary wave equation analyses using the GRLWEAP program (1), performed prior to mobilization at the site, indicated that the proposed Conmaco hammer (with its variable stroke) was capable of driving both pile sizes of all three types to targeted depths and anticipated capacities without pile overstressing.

The installation and restrikes of all eleven piles were monitored using a Pile Driving Analyzer (PDA) according to the Case Method procedures (2). Dynamic measurements of strain and acceleration were taken four feet below the head of each pile. Two reusable strain transducers and two piezoelectric accelerometers were bolted at opposite sides of each pile to monitor and minimize (by averaging) the effects of non-uniform hammer impacts. Strain and acceleration signals were conditioned and converted to force and velocity records by the PDA. Figure 2 shows pile head records of force and velocity (multiplied by pile impedance) under hammer blows from the end of driving of Piles 2A, 2B, and 2C. Dynamic records from the end of driving of a 30-inch (Pile 1A) and a 24-inch pile (Pile 3A) are presented in Figure 3. Illustrated in Figure 4 are plots of pile head dynamic records from the end of driving and beginning of restrike, five days after installation, of Pile 3B.

In the field, the PDA interpreted measured dynamic data according to the Case Method equations. The data was evaluated for pile driving stresses (compressive and

PILE	SIZE (IN)	LENGTH (FT)	PEN (FT)	BLOW COUNT (BL/FT)	STROKE (FT)	EMX (K-FT)	CSX (KSI)	TSX (KSI)	FMX (KIPS)	STATIC CAPACITY TOTAL (KIPS)	STATIC CAPACITY SKIN (KIPS)	STATIC CAPACITY TOE (KIPS)	SOIL DAMPING SKIN (S/FT)	SOIL DAMPING TOE (S/FT)	SOIL QUAKES SKIN (IN)	SOIL QUAKES TOE (IN)
1A	30	84	63.5	163	4	55.5	2.5	1.4	2250	1330	189	1141	.26	.06	.08	.42
2A	24	80	54.9	110	4	47.5	2.3	0.7	1330	1264	207	1057	.12	.06	.10	.37
3A	24	83	58.1	116	4	57.0	2.9	1.0	1650	1355	242	1112	.10	.05	.12	.41
4A	30	89	65.9	106	4	59.0	2.7	1.2	2450	1376	201	1175	.20	.08	.10	.41
5A	30	87	66.9	91	4	67.0	3.0	1.1	2700	1563	403	1160	.15	.09	.11	.30
2B	24	74	51.9	16	4	55.5	2.6	0.8	1520	640	186	454	.09	.07	.12	.61
3B	24	78	53.8	15	2	33.0	1.8	0.7	1015	354	78	276	.12	.03	.13	.80
4B	30	84	57.9	18	2	30.0	1.6	0.8	1450	346	87	259	.11	.06	.10	.68
2C	24	68	45.1	12	2	37.5	2.2	0.6	1245	240	210	30	.12	.08	.13	.50
3C	24	68	44.3	5	2	31.0	2.0	0.7	1180	75	36	39	.20	.16	.10	.60
4C	30	68	46.1	6	2	26.5	1.4	0.5	1280	92	78	14	.28	.12	.10	.11

PEN ... Pile penetration below mudline
EMX ... Maximum transferred energy to pile head
CSX ... Maximum compressive stress at pile top
TSX ... Maximum pile tension stress throughout pile driving
FMX ... Maximum compressive force at pile top

TABLE 1 Pile driving data and dynamic testing results
(For End of Initial Driving - EOD)

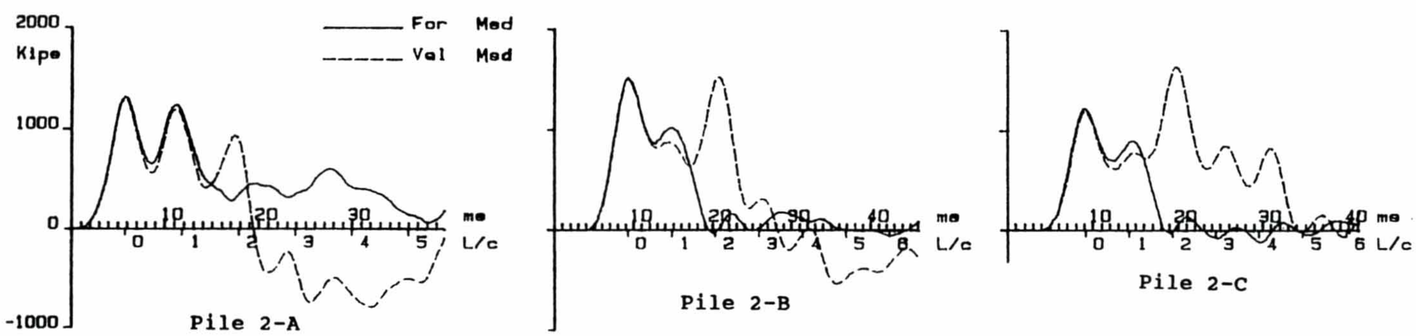

FIGURE 2 Pile head records;
Force vs Velocity, Site 2 @ EOD

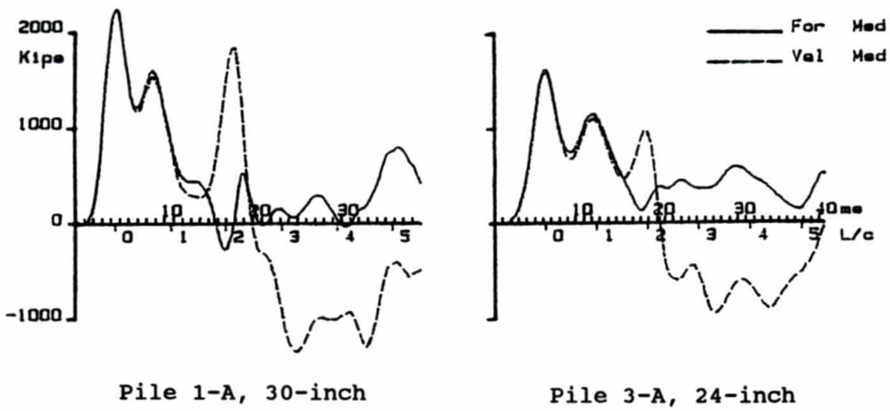

FIGURE 3 Pile head records;
Force vs Velocity, Piles 1A and 3A @ EOD

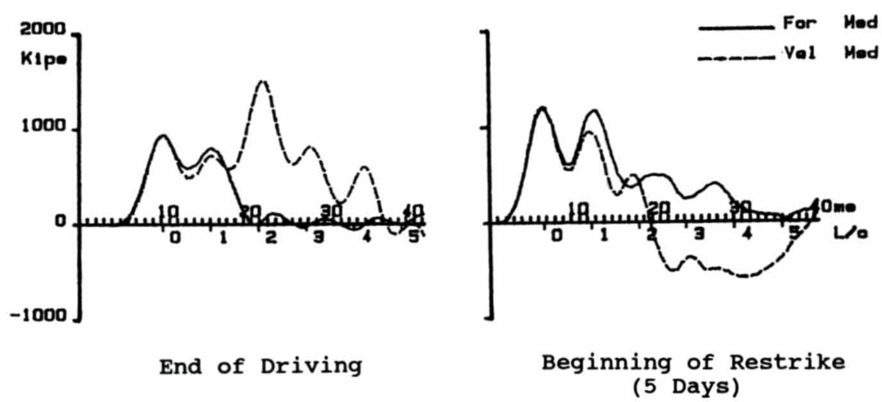

FIGURE 4 Pile head records;
Force vs Velocity, Pile 3B @ EOD and BOR

tensile), structural integrity, and static bearing capacity. Hammer-driving system performance was also investigated. Field measured dynamic data was additionally analyzed using the CAse Wave Analysis Program (CAPWAP) which is an analytical procedure performed interactively between the engineer and the computer program using a micro-computer (3). This method is used to compute soil resistance forces and their distribution using pile head force and velocity measurements recorded in the field in a wave equation type procedure. Results from a CAPWAP analysis include comparisons of measured with the corresponding computed pile force/velocity records. Numerically for each segment (approximately 5 ft) of the pile, ultimate static resistance, soil quake and damping factors are tabulated. Also included in the results is a pile head and toe load-set relationships computed from static test simulations. Figure 5 presents a typical CAPWAP analysis plotted results (end of driving of Pile 1A). A total of 32 CAPWAP analyses were performed on data from the end of driving and restrikes of all test piles. Dynamic testing results during pile installations are summarized in Table 1 and all dynamic analysis results are discussed below.

During installations, measured pile stress wave speeds averaged 12,500 ft/s which corresponds to a dynamic elastic modulus of 5055 ksi with a material unit weight of 150 pcf. This dynamically determined elastic modulus under loading rates between 500 to 1000 kips/ms is an average 20% higher than that determined from concrete cylinder crushing tests performed at the day of driving each pile.

The maximum compressive stress at pile heads during installation averaged 1.8 and 2.7 ksi with hammer strokes of 2 and 4 ft, respectively while the allowable stress was calculated to be about 3.6 ksi. Pile shaft tension stresses averaged 0.7 ksi with 2 ft ram strokes and 1.1 ksi (but reached 1.4 ksi for Pile 1A) with 4 ft strokes as compared to the calculated allowable stress in tension of about 1.2 ksi. During restrikes, compressive stresses were slightly higher and tension stresses substantially lower than those during initial driving. Dynamic data from all piles did not reveal indications of pile damage below gages, however, minor spalling did occur at the top of several piles.

While on short stroke (2 ft), the hammer-driving system delivered an average of 29 kip-ft of energy to pile heads and with 4 ft stroke it delivered an average transferred energy of 57 kip-ft. These energy transfer values correspond to transfer efficiencies of 48% when compared to the corresponding hammer rated energies. When comparing this energy transfer efficiency value to many others obtained on projects under similar conditions, it indicates a hammer-driving system performance in the top 35% of the sample. It was found that the injection of water into the upper side of the pile cap decreased pile head transferred energies by 5 to 10%, while shutting the water off increased the energy by a similar percentage.

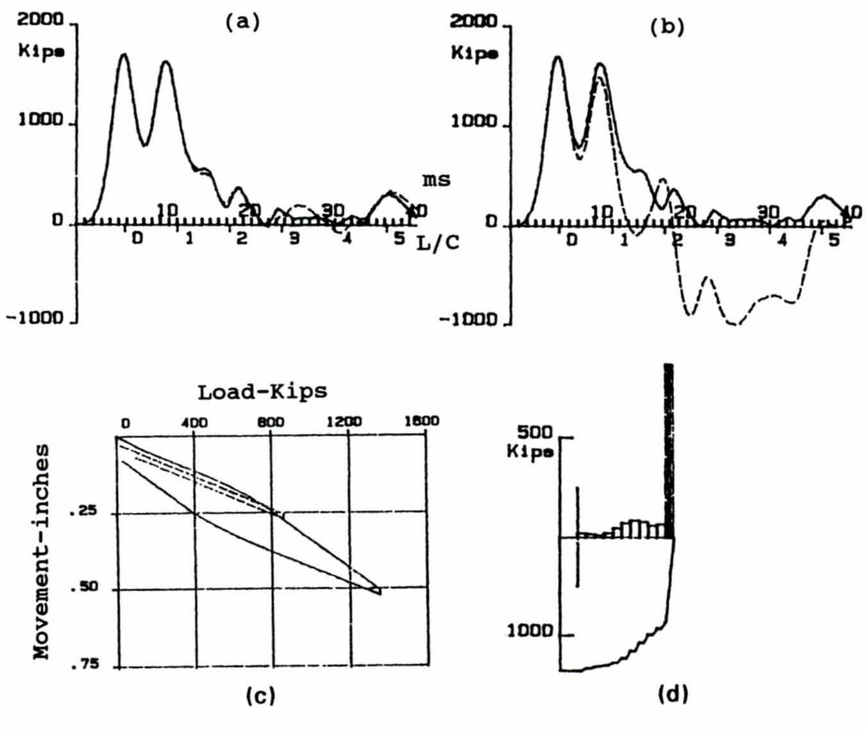

FIGURE 5 Typical CAPWAP analysis output; Pile 1A
(a) Measured and computed forces
(b) Measured force and velocity
(c) Load vs movement at pile head
(d) Resistance distribution and forces in pile shaft at ultimate resistance

For determination of pile static capacities, soil resistance distributions and dynamic variables, CAPWAP analyses were performed with dynamic data representing hammer blows from the end of driving and beginning of restrikes of all piles. For restrikes that consisted of a significant number of blows resulting in notable pile movement. End of restrike data was also analyzed. Comparisons show that PDA field calculated capacities were, on average, within 6% of CAPWAP computed values. Table 1 lists end of driving pile static capacity (total, shaft and toe resistances), soil damping and quake values along pile shafts and under pile toes for each test pile. As expected, A piles had the most end of drive capacity (average 1378 kips) and C piles the least (average 136 kips) with B piles in-between (average 447 kips). Dynamic testing during restrikes were performed to assess time dependent pile capcity changes. In all cases, pile capacities increased with time. End of driving blow counts of the A piles were generally over 100 BPF with higher values encountered at the beginning of restrikes. High pile driving resistance means small pile sets under hammer blows preventing full mobilization of soil resistance. A method of superpositioning, assuming no change in pile toe resistance with time, was employed as illustrated in Figure 6 for Pile 2A. The figure presents the CAPWAP calculated pile static capacity and shaft and toe resistances at the end of driving and during restrikes. At the beginning of each restrike, the hammer was unable to cause sufficient pile movement to mobilize maximum pile resistance, therefore the toe resistance from the previous end of driving analysis was added to beginning of restrikes shaft resistance to compute total pile capacity. Interestingly, at the end of the five day restrike (the restrike consisted of 38 hammer blows), the total pile driving resistance was the same as that at the end of initial driving and pile resistance magnitude and distribution were almost identical (within 2%) to those at the end of driving. Due to the low blow counts at the end of driving and during restrikes of the B and C piles, pile capacities were always mobilized and increases in values were entirely due to increases in shaft resistances.

CAPWAP computed shaft resistances for the B piles are plotted as a function of time (log time scale) along with results (according to Davisson's failure criteria) of uplift static loading tests in Figure 7. Data analysis indicates a linear increase in piles shaft resistance and an uplift static capacity that is, on average, 76% of compression shaft resistance. Due to the very low driving resistance of the C piles and the fact that static loading tests were not run to failure on almost all of the A piles, similar comparative analyses were not performed for these piles.

5. STATIC LOADING TESTS

5.1 Procedure

All eleven piles were subjected to uplift static loading tests during the month of December. Four, 18-inch diameter steel pipe reaction piles were used at each single test pile site and eight piles were used at each three test pile sites. Test piles were cut off and threadbars were exposed (4 and 6 for 24- and 30-inch piles, respectively) after the working platform was put into place. The load test frame consisted of a pair of cross beams supported on the reaction piles and twin girders placed onto the cross beams, over the test pile. The threadbars were then extended and connected to the two 600 kips (1200 kips total) hydraulic jacks which were placed on the test girder. Tension loads were applied in increments of approximately 5% of each pile's estimated (from CAPWAP) capacity. Maximum test loads were based on 80% of the maximum threadbar capacity of each pile size (i.e., 600 kips for 24-inch and 900 kips for 30-inch piles). Loads were removed in increments of 20% for rebound readings.

Three dial gauges (read to 0.001 inch) were placed at the top of the pile to measure top displacement. Dial gauges were also placed on the steel telltale rods to measure differential pile movements at various levels. A wire line and mirror system was additionally used to check dial gauge readings, and a remote platform was established to verify that the reference system was unaffected by test loadings.

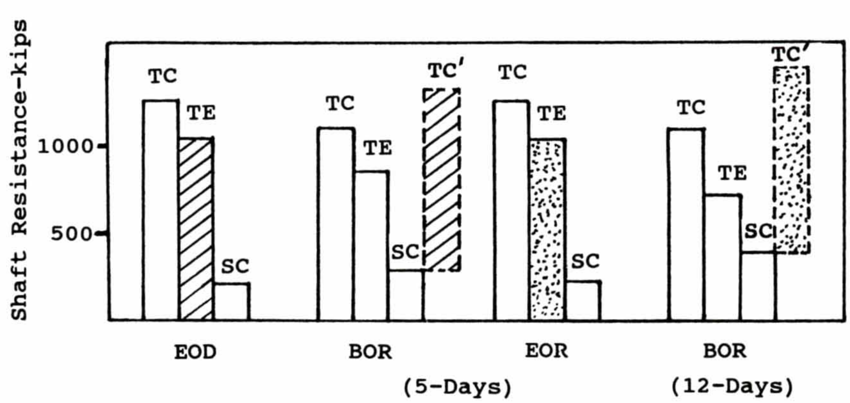

FIGURE 6 Superpositioning of CAPWAP data; Pile 2A where:
TE = Total capacity
TE = Toe capacity
SC = Shaft capacity

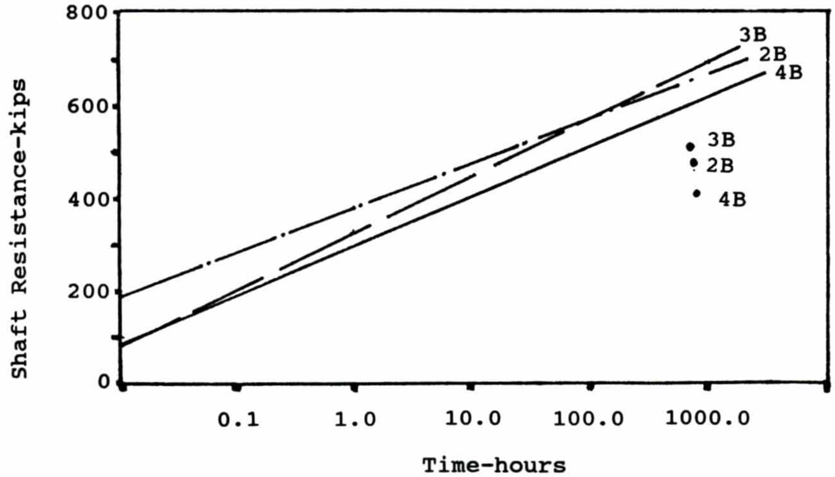

FIGURE 7 Shaft Resistance vs Time plotted with corresponding uplift shaft capacities

5.2 Results

Load versus displacement curves were plotted from which failure loads for each pile could be determined. As an example, Figure 8 presents plots of pile head load vs movement for A-piles,B-piles and C-piles, respectively. Five different methods were utilized to define failure loads. These methods were:

* Davisson's Method [elastic elongation + 0.15" + D/120]
* Canadian Method [elastic elongation + D/30]
* Tangent Intersection Method
* Specific Displacement [elastic elongation + 0.25"]
* Specific Displacement [elastic elongation + 0.10"]

Where D is pile side dimension.

Although meant to be used for compression static loading test data interpretation, the methods listed above were employed unmodified due to the lack of a universally accepted procedure for uplift static load test results assessment. It is recognized in particular, that the "D," factor in the Davisson and the Canadian Methods probably should be disregarded. Without that factor, the Davisson failure load would be equal to elastic elongation +.15 inch displacement which is between the two specific displacement methods applied. The Canadian Method would not be applicable. With it, the displacement criteria for Davisson's Method are elastic elongation +.35 inch or .40 inch for 24 inch or 30 inch square piles respectively. For the Canadian Method, displacements are elastic elongation +.80 inch or 1.00 inch for 24 inch and 30 inch piles respectively. It was decided to apply these methods in their common form to allow examination of a broader range of displacement criteria. With the exception of Pile 2A, all other A-type piles did not fail by any of the these methods. Load-movement curves for A piles were extrapolated using test data and patterns of displacements in failed Pile 2A. Figure 9 illustrates the application of these methods on the load vs displacement plot for Pile 2A.

The gross failure loads (including pile weights) produced by the above methods are listed in Table 2 along with the number of days elapsed between installation, redriving and testing. The results with Davisson's Method were selected to represent the piles' ultimate capacity in final design. Total pile top displacements associated with the application of this method were between .50 and .70 inch which was believed to be reasonable for an ultimate condition. Table 3 presents net failure loads (excluding pile weights) using this method for all piles. The table shows that the 30-inch A piles had the most capacity and the 24-inch C piles the least; inconsistencies, however, include the facts that the 30-inch B pile had less capacity than the 24-inch B piles, and that 24-inch A and B piles had about the same capacities.

5.3 Data Analysis

Predicted pile capacities were calculated using Nordlund's method for cohesionless soil intervals and the alpha method for cohesive soil intervals (4). These methods include a number of factors which require some judgement, particularly the selection of an alpha factor and the soil shear strengths. The difficulties associated with the selection of an alpha factor for medium to stiff clays are discussed in the literature (4). The shear strengths results from 7 undisturbed, field vane shear tests in the lower portion of Layer I varied between 2.08 and 4.02 ksf with an average value of 3.10 ksf. In those tests the ratio of undisturbed to disturbed strengths was 2.4. The results of thirteen laboratory unconsolidated, undrained triaxial shear strength tests in that same soil interval varied between .44 ksf and 2.5 ksf with an average of 1.24 ksf. Selection of a shear strength in these cohesive soils or the selection of a friction angle in cohesionless soils for evaluation of frictional resistance, introduces some level of probable variation when compared to field load test results. Estimates of pile capacities in Layer 1 were made using an alpha of .35 and an

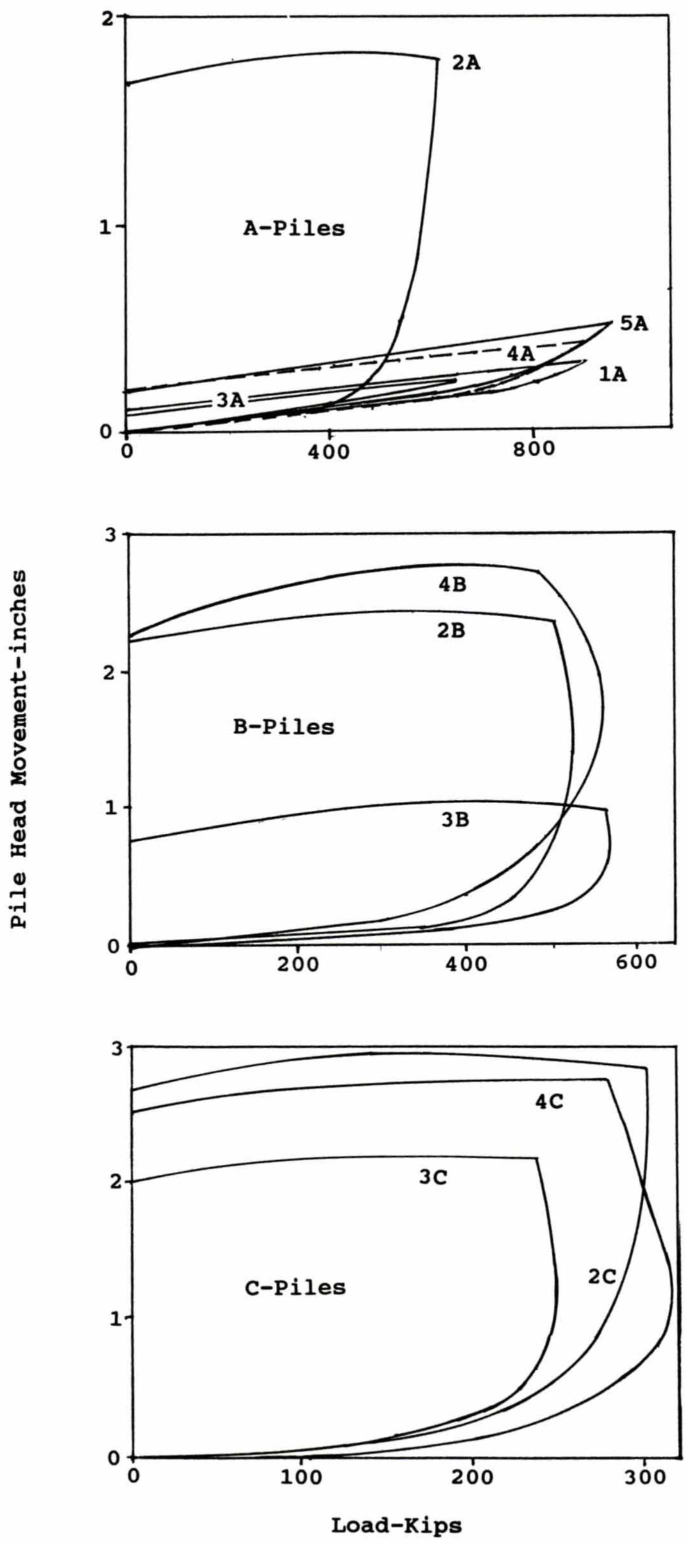

FIGURE 8 Pile Head Displacement vs Applied Load; For A-Piles, B-Piles and C-Piles

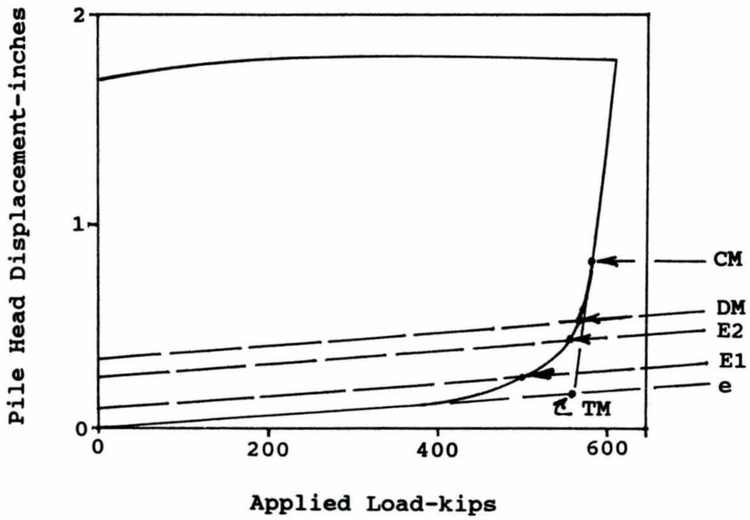

FIGURE 9 Typical Application of Failure Load Methods; Pile 2A, where:
e = Elastic elongation
E1 = e +.10 inch
E2 = e +.25 inch
DM = e +.15 inch + D/120 (Davisson's Method)
CM = e + D/30 (Canadian Method)
TM = Tangent Method

PILE	SIZE (inch)	TIME* (Days)	DAVISSON (Kips)	CANADIAN (Kips)	TANGENT (Kips)	e +.25" (Kips)	e +.10" (Kips)
1A**	30	50/43	1000	1080	1000	950	900
2A	24	36/24	570	590	560	560	500
3A**	24	37/31	610	610	600	590	550
4A**	30	49/36	950	1020	980	900	840
5A**	30	50/43	990	1050	1000	950	850
2B	24	36/24	485	515	490	470	440
3B	24	34/29	560	560	490	560	500
4B	30	49/36	430	530	450	380	360
2C	24	36/25	235	270	245	210	165
3C	24	35/30	220	240	170	200	160
4C	30	49/36	280	320	245	240	210

* Time between initial driving and testing/last restrike and testing
** Estimated failure load
e Elastic elongation

TABLE 2 Gross uplift failure loads by selected methods

PILE	SIZE (Inches)	NET FAILURE LOAD (Kips)
1A	30	950
2A	24	542
3A	24	580
4A	30	902
5A	30	938
2B	24	456
3B	24	532
4B	30	386
2C	24	208
3C	24	196
4C	30	242

TABLE 3 Net failure loads from uplift tests (Davisson's Method)

average shear strength of 3.0 ksf in the cohesive portion and an average friction angle based on Standard Penetration Test (SPT) data in the sandy portion. The same method was used to estimate capacity from Layers II and III since grain size analyses indicated they were also cohesionless. Failure loads for C-piles using the Davisson criteria were, on average, 73% of the computed estimates for pile ultimate frictional resistance. For piles 2B and 3B, the the net failure load was 123% of the computed ultimate resistance. Pile 4B is unusual in that this ratio was 56%. It is suggested that the variation in the C-piles may be attributable to the selection of an alpha factor or a shear strength for computation of a capacity. It is also suggested that for the B-piles, the higher ratio could be attributable to some type of cementation of the calcareous soils in Layers II and III. When these layers were treated as cohesionless soils, computation of their capacity was considerable underpredicted.

Unit soil adhesion values were computed for each soil layer using net failure loads from uplift tests and embedment lenghts in Layers I, II, and III from Piles A, B, and C at Sites 2, 3, and 4. Adhesion values for Layer I was determined from C piles. Unit adhesion for Layer II was calculated by subtracting the product of the unit adhesion and the estimated penetration in Layer I from the failure loads of the B piles. Similarly, calculation of an independent unit adhesion for Layer III from the A piles yielded unreasonable results. This was attributed to the minimal amount of penetration in this very dense layer. A reasonable match was obtained when the penetration lengths in Layers II and III were combined and a corresponding adhesion was determined.

An average adhesion value of 0.56 ksf was obtained for Layer I, and an average adhesion of 4.54 ksf was obtained for pentration into Layers II and III. These average adhesion values were also used to compute uplift capacities of Piles 1A and 5A. Results agreed within 10% of the measured values from the load tests (using Davisson's failure load). These adhesion values appeared to be representative of the soils encountered and were recommended for use as ultimate values in determining estimated uplift pile capacities for final design on the project.

Data from telltale movements was analyzed for computing adhesion forces from differential pile elongations considering applied loads and pile properties. This analysis yielded unrealistic results that were deemed unusable. It was concluded that the lack of sensitivity of the telltales and the large pile area cross sections were among the reasons for failure of this approach.

6. CONCLUSIONS AND RECOMMENDATIONS

The following conclusions were arrived at from the results of dynamic and static load tests at this site:

a) Dynamic testing can be used to evaluate pile capacity increases in skin friction due to time related increases in pile-soil adhesion.

b) The method of "superpositioning" can be used with CAPWAP results to determine the total capacity on high capacity piles which exhibit little pile toe movement when restruck.

c) The injection of cooling water at the pile hammer cushion during driving reduced energy which would otherwise be delivered to the pile by 5 to 10 percent.

d) Taking into account time factors when determining capacities from the uplift load tests, the ultimate test load on "B" piles determined by Davisson's method as described in this program was, on average, 76 % of the CAPWAP predicted compressive skin friction.

e) Prediction of frictional resistance based on generally accepted computational methods provided erratic and inconsistent results for the "B" and "C" piles. This suggests the need for uplift testing on projects where tension loads are significant in design or the use of appropriate factors of safety in other cases. The use of dynamic testing for this purpose offers potential that should be explored further.

f) For design at this site the recommended ultimate adhesion values for uplift capacity on piles was 0.56 ksf in Layer I and 4.54 ksf in Layers II and III.

g) Telltales did not provide reliable data for use in determining load distribution. This was attributed to several factors particularly,the sensitivity of calculations to the large pile area and the level of sensitivity in telltale data.

7. ACKNOWLEDGMENTS

In addition to their own organizations, the authors would like to acknowledge the encouragement and support of the Florida Department of Transportation (Bartow and Tallahasse Geotechnical Engineers' Offices) and of Misener Marine Construction, Inc. during the field work and in preparing this manuscript.

8. REFERENCES

1. Hussein, M., Rausche, F., and Likins, G., "Wave Equation Analysis Of Pile Driving: Methodology and Performance," Sixth National Conference on Microcomputers in Civil Engineering, University of Central Florida and ASCE, Orlando, Florida, 1988.

2. Likins, G., Hussein, M., and Rausche, F., "Design and Testing of Pile Foundations," Third International Conference on the Application of Stress Wave Theory to Piles, Bengt Fellenius editor, Ottawa, Canada, 1988.

3. Rausche, F., "Soil Response From Dynamic Analysis and Measurements on Piles," Ph.D. Thesis Case Western Reserve University, Cleveland, Ohio, 1970.

4. Vanikar, S.,N., "Manual on Design and Construction of Driven Pile Foundations," FHWA-DP-66-1,Revision 1, April, 1985

9. APPENDIX

1 ft = 0.305 m, 1 inch = 2.54 cm, 1 kip = 4.45 kN, 1 ksi = 6.89 MPa, 1 kip-ft = 1.36 kJ

YPLOT, NOTE02

γ: Tension Over Compression Conversion Factor

Reference A:

Chinese Specifications DB62/3065, 2013

(Procedure in Determination of Qu Ultimate Value, Clause 6.3)

Soil Type	**Sand**	**Clay**	**Rock**	**Mix**
γ Factor	0.7	0.8	1.0	take average

Reference B:

Tech Paper Stress Wave Conference, 2008

(CAPWAP for Uplift Resistance Evaluation)

Soil Type	**Sand**	**Clay**	**Rock**	**Mix**
γ Factor	all use 0.8			

Document NOTE02, Reference A

Chinese Specifications DB62/3065, 2013

(Procedure in Determination of Qu Ultimate Value, Clause 6.3)

Specifications on Bi-direction Pile Load Test

using

YJACK System on Bored Piles

Translated from

Chinese Specifications DB62/3065-2013

(Procedure in Determination of Qu Ultimate Value)

Published By

YJACK Technology, Malaysia

(www.YJACKpiletest.com)

on

2017 June 20

6 测试数据的分析与判定

6.1 自平衡法试验数据分析

6.1.1 确定单桩竖向极限承载力时，应绘制 $Q_u^s-s_s$、$Q_u^x-s_x$、$s_s-\lg t$、$s_x-\lg t$ 曲线，需要时也可绘制其他辅助分析所需曲线。

6.2 Q_u^s 和 Q_u^x 的确定

6.2.1 根据位移随荷载的变化的特征确定：对于陡变型 $Q_u^s-s_s$、$Q_u^x-s_x$ 曲线，取其发生明显陡变的起始点对应的荷载值。
6.2.2 根据位移随时间的变化特征确定：上段桩取 $s_s-\lg t$ 曲线尾部出现明显向上弯曲的前一级荷载值，下端桩取 $s_x-\lg t$ 曲线尾部出现明显向下弯曲的前一级荷载值。
6.2.3 出现第 5.3 条第 2 款情况，取前一级荷载值为极限承载力。
6.2.4 对缓变型 $Q_u^s-s_s$、$Q_u^x-s_x$ 曲线，按位移值确定极限承载力值，Q_u^s 取对应于向上位移 s_s=40mm 对应的荷载值；Q_u^x 可取 s_x=0.05D 对应的荷载值。

6.3 单桩极限承载力的推定

6.3.1 荷载箱位于平衡点或中性点位置时，推定单桩竖向抗压极限承载力可按下列公式计算：

$$Q_u=\frac{Q_u^s-W_s-W_p}{\gamma}+Q_u^x \qquad (6.3.1)$$

式中：Q_u——单桩竖向抗压（拔）极限承载力值；
W_s——上端桩桩身自重；

W_p——有效堆载重量。当反力不足时，也可在桩顶增加堆载配重；
γ——荷载箱上段桩侧阻力修正系数，根据荷载箱上部土的类型确定，粘性土、粉土取 0.8，砂土、碎石土取 0.7，岩石取 1.0，若上部有不同类型的土层，γ 取加权平均值。

6.3.2 单桩竖向抗拔极限承载力可按下列公式计算：

$$Q_u=Q_u^s \qquad (6.3.2)$$

6.3.3 荷载箱位于桩底位置时，推定单桩竖向抗压极限承载力可按下列公式计算：

$$Q_u=\frac{Q_u^s-W-W_p}{\gamma}+Q_{pk} \qquad (6.3.3\text{-}1)$$

$$Q_{pk}=\psi_p\times Q_u^x\times\left\{\frac{A_p}{A}\right\} \qquad (6.3.3\text{-}2)$$

式中：Q_u——单桩竖向抗压（拔）极限承载力值；
Q_{pk}——桩端极限阻力推定值；
W——桩身自重；
A——荷载箱承压底板面积；
A_p——桩端面积；
ψ_p——大直径灌注桩端阻力尺寸效应系数，按《建筑桩基技术规范》JGJ 94 中相关规定取值。

6.4 单桩竖向极限承载力统计值的确定

6.4.1 参加统计的测试桩不少于 3 根时，当满足极差不超过平均值的 30%时，取其平均值作为单桩竖向抗压极限承载力。
6.4.2 当极差超过平均值的 30%时，应分析极差过大的原因，结合工程具体情况综合分析，必要时可增加测试桩数量。
6.4.3 测试桩数量少于 3 根时，应取低值。

Symbol:	Qu(s) = Qu(up); ultimate load Qu upward	s(s) = s(up); displacement upward
	Qu(x) = Qu(dn); ultimate load Qu downward	s(x) = s(dn); displacement downward
	lgt = logt; log time	W(s) = W(up); pile weight above jack
	γ; tension over compression factor	W(p); surcharge load for insufficient friction

6 Bi-Directional Pile Load Test Analysis Method

6.1 Bi-Directional Pile Load Test Plots

6.1.1 The report shall present the plots for Qu(up)-s(up), Qu(dn)-s(dn), s(up)-logt, s(dn)-logt and other plots.

6.2 Determine Qu(up) and Qu(dn)

6.2.1 Determine ultimate load from large displacements:
Based on Qu(up)-s(up) and Qu(dn)-s(dn) plot, determine the Qu from the significant displacement point.

6.2.2 Determine ultimate load from the stability of the displacements:
Based on s(up)-logt and s(dn)-logt plots, select Qu from the loading step prior to the instability of the displacements for more than 2 hours.

6.2.3 Determine ultimate load from 5x displacements
In any loading steps, when the displacements larger than the early loading step 5 times (5x), then select Qu in loading step prior to 5x displacement.

6.2.4 Determine ultimate load from s(up) > 40mm or s(dn) > 0.05D displacements
In any loading steps, when s(up) > 40mm displacement, determine the Qu when reach s(up) = 40mm; or, when s(dn) > 0.05D, determine the Qu when reach s(dn) = 0.05D.

6.3 Ultimate Load, Qu

6.3.1 The final ultimate load after correction shall be computed as following:

$$\text{Qu(compression)} = \frac{\text{Qu(up)} - \text{W(up)} - \text{W(p)}}{\gamma} + \text{Qu(dn)}$$

(γ = 0.7 for sand; 0.8 for clay; 1.0 for rock)

6.3.2 The tension load can be approximately as:
Qu(tension) = Qu(up)

Document NOTE02, Reference B

Tech Paper Stress Wave Conference, 2008

(CAPWAP for Uplift Resistance Evaluation)

Use of CAPWAP for uplift resistance evaluation of wind energy Tower piles

Teferra, W. & Saavedra, M.R.
GRL Engineers, Inc., Chadds Ford, PA, USA

Echaniz, P.
CME Assoc., (EGS Associates), Atlantic City, NJ, USA

ABSTRACT: Structures founded on piles derive their support from skin friction and toe bearing. For some structures piles are specified for the primary purpose of providing uplift resistance against forces of wind, flood and seismic loading. The magnitude of support provided by each pile is dependent on its penetration into the competent soil material. Dynamic testing and analyses of 14-inch diameter steel pipe piles installed for five wind-energy generating Towers located near the Atlantic City shore are described in this paper. The Towers are subjected to wind and potential flood loading. The soil conditions at the site consisted of approximately 48-ft (14.6 m) thick layer of fill and organic soils overlying medium dense to dense granular deposits. The fill and organic soils are determined to be unsuitable to provide uplift support for the structures. Only the section of the pile penetrated into the medium dense to dense granular materials would be considered to resist tension. Dynamic testing of several piles were performed and analyzed by CAPWAP® with emphasis on pile shaft resistance evaluation and its distribution along the length of the piles. The friction values contributed from the fill and organic soils were subtracted from the total friction calculated by CAPWAP in the evaluation of uplift pile capacity. In addition, consideration was given to the effect of Poison's ratio in calculating the final uplift resistance from compression loading. Several piles installed for the five wind-energy Towers were tested and evaluated by CAPWAP for both compression and uplift capacities. Based on the test and analysis results, recommendations were made regarding the minimum pile penetration into the soil strata considered to be competent in resisting both the required tension and ultimate compression loads. Results from CAPWAP analysis of the dynamic records established such information and provided confidence to the engineers in evaluating both the uplift and compression capacities of the piles.

1 INTRODUCTION

The project described in this paper consisted of the evaluation of pile foundation installed for five windmill structures constructed to generate 7.5 megawatt (MW) electric power. The windmill structures are located near the coast of Atlantic City in New Jersey, USA. It is the first windmill coastal farm in the United States. The project is predicted to produce approximately 19 million kilowatt-hours of emission-free electricity per year which is enough to power 2500 homes. Each windmill turbine is approximately 381 ft (117 m) tall. Considering loads from wind, wave forces and seismic loading, each windmill turbine is designed to be supported on 24 piles. Most of the piles are driven at a batter of 1:10 and are spaced equally in a circular layout. Based on structural and geotechnical considerations 14 inches (356 mm) outer diameter steel pipe piles with uniform wall thickness of 0.375 inches (9.5 mm) were selected for the project. The toe of each pile was fitted with a conical pile point. The pile driving contractor, Tuleya Pile & Foundation, Inc., used a Pileco D19-42 single acting diesel hammer to install the piles. This hammer has a ram that weighs 17.9 kN and is rated for a maximum energy of 57.6 kN-m.

In addition to providing support for compression loading, the piles are designed for the primary function of providing uplift support generated from lateral forces of wind, flood and seismic loading. Considering the subsurface conditions at the site, installation of the piles to soil strata that provide sufficient uplift is of primary challenge to the geotechnical engineers. The resistance along the pile shaft is dependent on the soil type, strength and pile penetration into competent soil. This resistance force is calculated from dynamic measurements of force and velocity with emphasis on computing the shaft resistance by CAPWAP® (CAse Pile Wave Analysis Program) analysis. Test results of several piles installed at five windmill locations are presented in this paper. In addition, both static compression and tension load testing at windmill Tower 4 location were performed to check the adequacy of the piles to resist the required ultimate compression and tension loads.

2 PROJECT LOCATION AND DESCRIPTION

The Atlantic County Utilities Authority (ACUA) Wind Energy Farm is located in Atlantic City, New Jersey, USA. The owners, Jersey Atlantic Wind LLC in partnership with the original developer Community Energy, Inc. (currently a subsidiary of Ibedrola, S,A.), constructed a total of five windmills providing 1.6 megawatts each. The Tower hubs are 80.6 meters high and 4.3 meters in diameter. The blades are 34.3 meters long for a total height to tip of blade of approximately 117 meters. The tips travel at approximately 75 kilometers per hour.

3 GEOLOGY

Atlantic City occupies the northern end of Absecon Island, which is a classic barrier beach type geologic landform. The island was formed by deposition of sands by littoral drift currents and the development of tidal marshes in sheltered areas on the inner shore during the geologically recent period of rising sea level since the last glacial age. The ACUA/ Community Energy, Inc. Wind Energy Farm project area appears to be in a zone of alternating active beach and back bay marsh type deposition. Thick strata of marsh deposits were encountered between strata to loose to medium dense sands to depths of 13 to 15.5 meters. The barrier beach and tidal marsh was deposited over more ancient coastal plan sediments. The uppermost of the geologic strata is the Cohansey Formation consisting of medium to dense sands with frequent lenses of stiff inorganic clays and silts. These appear to have been encountered at depths of approximately 15.0 to 19.5 meters in the borings. The underlying formations extend to great depth and consisted of interbedded sands, gravels, marls, clays and silts.

4 SUBSURFACE DESCRIPTION

Several boring logs were taken at the project site. The upper layers consisted of peat, and organic silt to a depth of 14.6 m (48 ft) and the depth below the organic silt was described as gray sand with silt and gravel to the boring termination depth of 24.4 m (80 ft). The Standard Penetration Test (SPT) in the bottom strata ranged between 29 to 91 blows per 30 cm (29 to 91 blows/ft). The upper 14.6 m of the soil is considered unsuitable of supporting uplift resistance. Only pile penetration depth in the gray sand with silt and gravel is considered suitable to support uplift resistance generated from the wind, storm and seismic loading. A subsurface section depicting the general soil stratigraphy at the site is shown in Fig. 1.

5 DYNAMIC PILE TESTING OF WINDMILL TURBINE FOUNDATION

Methods to measure force and velocity near the pile top have become a routine practice. Several piles at the five windmill turbine locations were tested dynamically and the measured force and velocity records were analyzed to check both the uplift resistance and compression capacity of the piles. Testing consisted of attached two strain transducers and two accelerometers at approximately 1 m from the top of the piles. During impact driving, the force and velocity records were processed to yield pile driving stresses, hammer energy transferred to the piles, hammer stroke, and other quantities. At the time of testing, the capacity of a pile is computed from one dimensional wave theory referred as the Case Method technique. This method produces the total driving resistance, i.e., the sum of static and dynamic resistance forces. However, the dynamic resistance should be separated from the total computed resistance forces to arrive at the static soil resistance. Using CAPWAP analysis, the total static capacity for each test pile was computed and the result was split between shaft resistance and its distribution along the embedded length of the pile and pile toe bearing value. Records collected during initial driving and during restrike testing after the dissipation of pore water pressure, were analyzed. For long term capacity evaluation, analysis is based on restrike records of the force and velocity obtained several days after the completion of initial driving.

6 CAPWAP METHODOLOGY

Measuring both force and velocity records near the pile top are well established. However, the static and dynamic soil resistance forces plus all forces and motions below the pile top are unknown. In the CAPWAP method of analysis, it is possible to analyze a pile under the action of either the force record or velocity record or their average (which is the force in the downward wave) and an assumed soil model and compare the computed record to the unused upward wave. The difference between the measured and computed curves leads an engineer to conclusions regarding the differences between the actual soil behavior and assumed set of soil parameters. Modifications of these parameters leads to a better match and a subsequent iteration.

Therefore, CAPWAP is a signal matching procedure which uses the pile top force and velocity measurements generated during hammer impact. In this numerical computation, the pile is divided into a

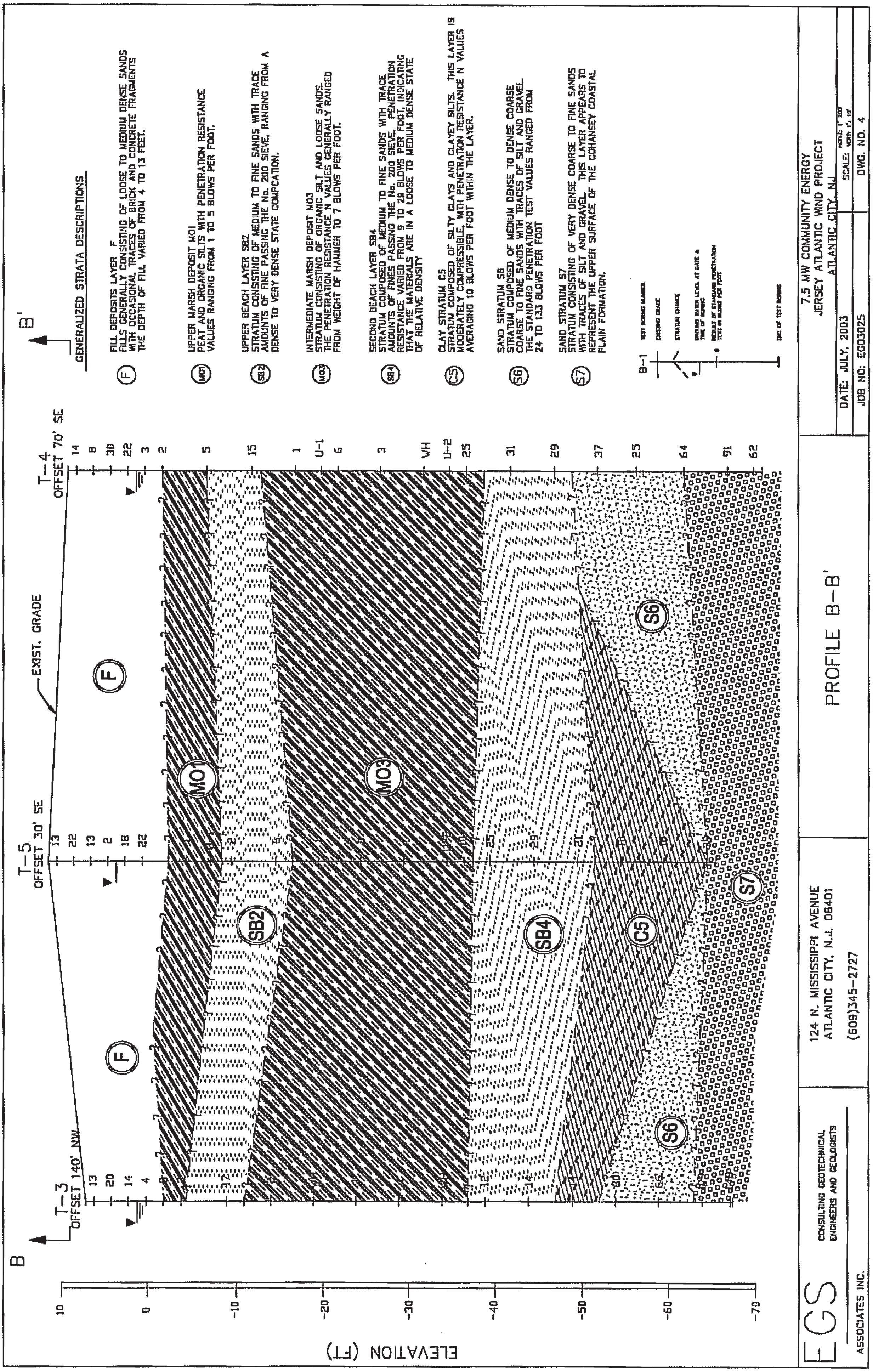

Figure 1. Generalized strata descriptions.

series of segments of uniform properties with soil resistance forces acting at each embedded pile segment. The soil model is considered as an elasto-plastic spring and as a linear dashpot described by three parameters: ultimate resistance, quake and viscous damping factor. In the iteration process, mainly these three parameters are varied in an effort to obtain a good match between the measured and computed forces.

In the present project, the measured downward travelling waves obtained from either initial drive or restrike testing of the piles were input to the CAPWAP program. Several iterations were made until a good match between the downward and upward travelling waves was obtained. The iteration was stopped when the match could not be improved further. The resulting soil element resistance forces were summed to yield the total refined capacity of the piles. The pile toe soil element resistance was then subtracted from the total resistance to yield total skin friction and its distribution along the pile shaft.

7 RESULTS FROM CAPWAP ANALYSES

Several piles located at the five sites were dynamically tested. These piles were driven to penetrations and blow counts indicated in Tables Nos. 1 and 2. The project specification requires that each pile must be driven to an ultimate compression capacity of 1877 kN and an effective uplift capacity of 347 kN. Per geotechnical consideration, the piles should have a minimum embedment of 8.2 m into the lower soil strata, described as a medium dense to dense layer, to resist uplift from lateral force of wind, storm and seismic loading.

The output from CAPWAP includes a refined total pile capacity split between shaft resistance and pile toe bearing. The results from the analysis indicated that the required ultimate compression capacity of the piles could easily be achieved. For uplift resistance evaluation, data from both initial driving and restrike testing of several piles were analyzed to check if the required uplift resistance was satisfied. The total skin friction calculated by CAPWAP was reduced to account for the effect of Poison's ratio in computing tension resistance from compression loading. According to the practice of the first author, a reduction of the computed skin friction by 20% is generally applied to estimate uplift resistance. The upper fill and organic soils are considered unsuitable to provide uplift support. Therefore, the skin friction computed by CAPWAP in the upper layers had to be subtracted from the total skin frictional forces to yield uplift resistance in the lower 8.2 m of pile penetration. As stated above a reduction factor was applied to the calculated uplift resistance to arrive at the usable tension load.

8 EVALUATION OF THE TEST RESULTS

8.1 Towers 1 and 2

The results of the dynamic pile tests performed on five piles at Tower 1, and four piles at Tower 2 are summarized in Table 1. All test piles at Tower 1 were tested during restrike while the piles at Tower 2 were tested during both initial driving and restrike testing. The compression capacity of the piles in Tower 1 ranged between 1825 and 2114 kN, with total skin friction ranges of between 677 and 835 kN. The skin friction at the bottom 8.2 m penetration of the piles ranged between 477 and 716 kN. These values were computed from the force and velocity records obtained during compression loading by hammer impact, and had to be reduced to account for the effect the loading direction had on these results. Therefore, the applicable (effective) resistance values to support uplift ranged between 382 and 573 kN. These values were higher than the required uplift of 347 kN. The above results represent values obtained from restrike testing of the piles.

At the location of Tower 2, the compression capacity of the piles ranged between 1534 and 1860 kN at the end of initial driving. Restrike testing of the piles had to be performed in order to check the long term capacity of these piles. During restrike after 2 to 6 days, the capacities in compression increased and reached values higher than the required ultimate capacity of 1877 kN. Evaluation of tension resistance in the lower 8.2 m of the piles at Tower 2 was based on restrike records, except for pile TP208, which reached the required tension capacity during initial driving. Per CAPWAP analysis results, the three piles tested during restrike indicated tension capacities higher than the required value of 347 kN.

8.2 Towers 3, 4 and 5

Four piles including a Load Test Pile (LTP-1), and three reaction piles were tested at Tower 4 location. Three of the piles, except the load test pile LTP-1, were also tested during restrike a day after their initial driving. According to CAPWAP analyses results, all reaction piles except pile WT417 achieved the required ultimate compression capacity of 1877 kN at the end of initial driving. Pile WT417 reached its required compression capacity during restrike a day later. The uplift resistance, computed by CAPWAP for the lower 8.2 m penetration was lower than the required value of 347 kN for all piles tested within.

All piles in Tower 4 did not achieve ther required uplift capacity during restrike, except for reaction pile WT418 which achieved an uplift capacity of 367 kN. With longer waiting time, it is likely that the uplift resistance could be achieved. The empirical formula developed by Svinkin and Scov (2000); $\mathbf{R_U(t)/R_{EOD} - 1 = B(log_{10}(t) + 1}$ was utilized to estimate pile set-up. The computed compressive capacities, after one month and six months, indicated that pile

Table 1. Summary of Dynamic Pile Test Results

Test Piles at Windmill Towers 1 and 2

Project: Jersey Atlantic Windmill Towers
Location: Atlantic City, New Jersey

Hammers: Pileco D19-42 single acting diesel
Pile: 14"ODx0.375" (356 mm OD x 9.5 mm) with conical point

Pile Number	Final Depth Below Ground m	Reported Blow Counts blows/25 cm	Test Type	Results from CAPWAP Analysis Total Capacity kN	Total Shaft kN	(a) Friction at Lower 8.2 m of Pile kN	(b) Uplift Resistance 80% of (a) kN
TOWER 1							
TP123	21.2	80	RS	1895	783	679	543
TP113	16.8	100	RS	2114	678	488	390
TP104	16.8	90	RS	1886	677	519	415
TP108	17.1	120	RS	1873	835	716	573
TP119	17.1	70	RS	1825	743	477	382
TOWER 2							
TP216	22.1	40	ED	1534	447	317	254
	22.1	80	RS	1740	641	425	340
	22.8	120	RD	1890	653	451	360
TP201	21.7	80	ED	1775	535	470	376
	22.8	110	RD	1893	650	472	378
TP220	22.1	60	ED	1712	486	318	255
	22.1	80	RS	1912	695	537	429
TP208	22.0	80	ED	1860	531	462	370

Notation:ED —— End of Initial Driving; RS —— Restrike; RD —— Redrive(a) —— Friction at bottom 8.2 m of pile is considered effective from geotechnical consideration(b) —— 20% reduction for the effect of compression loading in estimating uplift

set-up increases capacity by factors of approximately 1.35 and 1.51, respectively. These factors could be applied to the uplift capacity obtained from the CAPWAP analyses in the pile segments within the granular strata beneath the organic deposits.

The LTP-1, tested during initial driving, indicated a compression capacity of 1882 kN which is higher than the required ultimate value of 1877 kN. The effective uplift resistance based on CAPWAP analysis of the end of initial drive record obtained on the LTP-1 was 291 kN which is lower than the required value of 347 kN. This pile was not dynamically tested during restrike.

Pile 309 at Tower 3 achieved the required compression capacity of 1877 kN at the end of initial driving while pile TP500 at Tower 5 achieved this capacity during restrike a day later. The uplift capacity considered effective, i.e., in the lower 8.2 m of pile penetration, was 420 kN for pile TP309 which is higher than the required value of 347 kN while pile TP500 achieved the same uplift capacity of 420 kN, during the restrike the test after the dissipation of the pore water pressure.

9 STATIC COMPRESSION AND TENSION TESTS

"Proof" static load tests of both compression and tension were however performed on the LTP-1 several days after the pile was initially driven. The compression load test was performed based on ASTM D1143 Standard Method of Piles Under Axial Compressive Load and the tension test based on ASTM D-3689 Method 7.5 Constant Time Interval Loading. The test pile sustained the required ultimate compression load of 1877 kN for 12 hours with gross settlement of 13.7 mm. The net settlement after removing the load was 3.9 mm. Applying the Davisson's Failure Limit, pile LTP-1 could fail at axial compression load of 2446 kN. The compression test curve is indicated in Fig. 2.

Table 2. Summary of Dynamic Pile Test Results

Test Piles at Windmill Towers 3, 4 and 5

Project: Jersey Atlantic Windmill Towers
Location: Atlantic City, New Jersey

Hammers: Pileco D19-42 single acting diesel
Pile: 14"ODx0.375" (356 mm OD x 9.5 mm) with conical point

				Results from CAPWAP Analysis			
Pile Number	Final Depth Below Ground m	Blow Counts Reported bls/25 cm	Test Type	Total Capacity kN	Total Shaft kN	(a) Friction at Bottom 8.2 m of Pile kN	(b) Uplift Resistance 80% of (a) kN
TOWER 3							
P309 Batter	19.5	400	RS	2250	715	525	420
TOWER 4							
RP2 Plumb	17.8	70	ED	1884	478	272	218
	17.8	200	RS	1988	534	372	298
WT418 Batter	19.2	100	ED	1888	429	302	242
	19.2	120	RS	1957	534	459	367
WT417 Batter	18.0	80	ED	1734	355	248	200
	18.0	120	RS	1895	507	374	300
LTP-1 Plumb	18.9	80	ED	1882	463	363	291
TOWER 5							
TP500 Plumb	23.4	50	ED	1736	568	425	340
	23.4	100	RS	1885	705	526	420

Notation:ED —— End of Initial Driving RS —— Restrike(a) —— Friction at bottom 8.2 m of pile is considered effective from geotechnical consideration(b) —— 20% reduction for effect of compression loading in estimating uplift

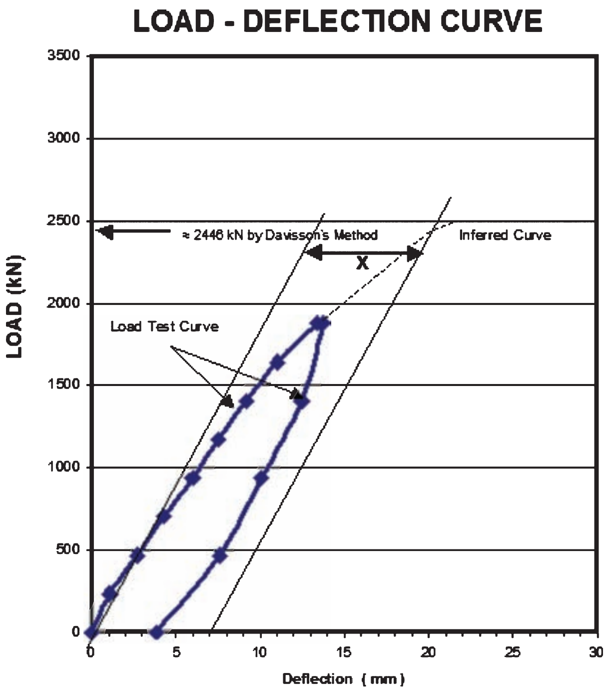

Figure 2. Static load test results in compression.

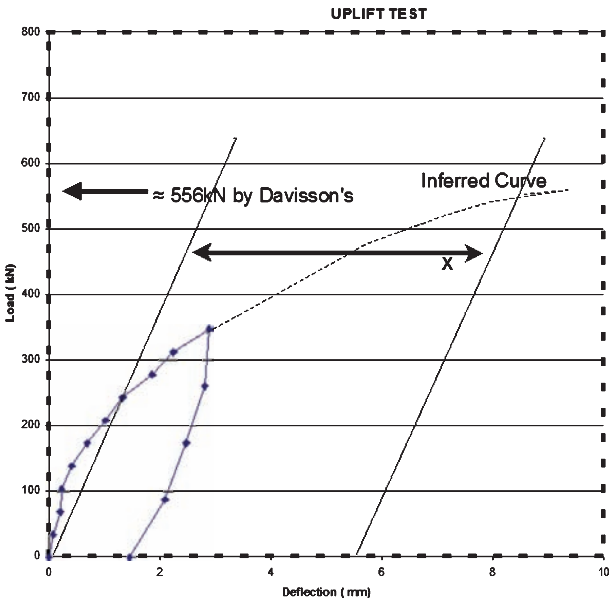

Figure 3. Static load test results in tension.

The same pile sustained a tension load of 347 kN for 12 hours with gross deflection of 2.9 mm. The net deflection after the load was removed was 1.45 mm.

Applying the Davisson's Failure Limit, the test pile would fail at a tension load of 556 kN. Results of the static test include the contribution of the resistance of the upper soil layer considered undesirable to support uplift. The static tension test curve is indicated in Fig. 3.

10 CONCLUSIONS

Several piles were dynamically tested during the installation of the foundation piles for the windmill structures at the coastal line of Atlantic City, New Jersey. Requirements for compression loading can be checked easily with routine dynamic pile testing. However, checking the uplift resistance of the piles against the forces of wind, flood and seismic loading was a major challenge. With the use of dynamic pile testing and subsequent analysis of the records by the CAPWAP analysis program, the total skin friction along the length of the piles was computed. It was necessary to reduce the computed shaft resistance in order to account for the effect of compression loading (Poisson's ratio effect) in establishing valid tension pile capacity. In addition, the soil resistance in the lower 8.2 m of pile penetration was considered effective in providing uplift resisting from forces of wind, storm and seismic loading of the structures. Some piles tested during initial driving indicated uplift resistance less than the required value of 347 kN in the lower 8.2 m of pile penetration, while most of the piles tested during restrike after a waiting period of between one and seven days had uplift resistance higher than the required value as indicated in Tables Nos. 1 and 2. The compression capacity of the piles was easily achieved during either initial driving or restrike after soil setup took place.

Pile LTP-1, located at Tower 4, indicated a CAPWAP computed compression capacity of 1882 kN and an uplift resistance of 291 kN at the end of initial driving. The uplift resistance represents 80% of CAPWAP computed tension capacity in the lower 8.2 m of pile penetration. This pile satisfied the compression requirement of 1877 kN at the end of initial driving. Both compression and tension static proof loads applied to this pile, after a few days of its initial driving, indicated that the pile could support at least 1877 and 347 kN, respectively. Although, the compression and tension static tests were terminated at proof loads of 1877 and 347 kN, respectively, failure loads in compression and tension of approximately 2447 and 556 kN, respectively, were projected from the static load test curves based on the Davison's Failure Limit.

Based on dynamic testing, both compression and uplift resistance of the piles were checked. An advantage was taken of the capability of the CAPWAP program to compute skin resistance forces at any location along the pile penetration. The shaft resistance calculated for selected soil layers within the penetration of the piles was used to check if that resistance could provide sufficient uplift or tension capacity. Based on the tests and analyses results, it was concluded that piles in Towers 1 and 2 should be installed to minimum penetrations of 17 m and 22 m, respectively, at blow counts of 32 blows per 10 cm with the hammer operating at an average stroke of 2.8 m. Similarly, conclusions regarding the installation of the production piles at Towers 3, 4 and 5 were made based on the PDA testing and CAPWAP analyses results. Piles at Towers 3 and 4 were to be driven to a penetration of at least 19 m to blow counts of 32 blows per 10 cm with the hammer operating at an average stroke of 2.8 m. The dynamic testing and CAPWAP analyses indicated that piles at Tower 5 required a deeper penetration of 24 m and that the blow counts at final driving should be approximately 32 blows per 10 cm with the hammer operating at an average stroke of 2.7 m at the end of driving. CAPWAP analyses provided valuable information to cost-effectively establish the above criteria and adequate installation of the piles supporting wind turbine Towers in unfavourable subsurface condition.

ACKNOWLEDGEMENTS

The authors gratefully acknowledge the following: Energy Works/Community Energy, Inc., A subsidiary of Iberdrola, S.A, Babcock & Brown, Garrad Hassan America, Inc., Garrad Hassan and Partners, Ltd., Barr Engineering Co., Paulus, Sokolowski & Sartor, LLC; Q West; TRC Solutions; P Sands; and M.A. Mortenson Co.

REFERENCES

ASTM D3689 "Method of Testing Individual Piles Under Static Axial Tensile Load," and ASTM D1143 "Standard Method of Testing Piles under Static Axial Compression Loads".

ASTM D4945-96 "Standard Test Method for high Strain Testing of Piles".

Axelesson, G., "Long Term Set-up of Driven piles in Sand" Doctoral Thesis, Division of Soil and Rock Mechanics, Department of Civil and Environmental Engineering, Royal Institute of Technology, Stockholm, 2000

Fung, W.K., Wong, C.T., and Wong, M.K. (2004). "Correlation Studies of CAPWAP and Static Load Test", Proceedings of The Seventh International Conference on the Application of Stresswave Theory to Piles.

Komurka, V.E., and Wagner, A.B. (2003). "Estimating Soil/Pile Set-up," University of Wisconsin – Madison, Wisconsin Highway Research Program # 0092-00-14. WHRP 03-05.

Liang, R.Y. and Yang, L. (2007). "Dynamic Pile testing technology: validation and implementation". Ohio Department of Transportation and Federal Highway Administration State Job No. 14794, Final Report FHWA/OH-2007-08.

Likins, G. and Rausche, F. (2004). "Correlation of CAPWAP with static load tests". Proceedings of The Seventh International Conference on the Application of Stresswave Theory to Piles.

Martel, D.W., and Klingberg, D.J. (2004). "Comparison of Dynamic and Static Testing Methods for Tension Capacity of Reinforced Concrete Piles". Proceedings of The Seventh International Conference on the Application of Stresswave Theory to Piles.

Poulus H.G. and Davis E.H. (1980). "Pile Foundation Analysis and Design", Wiley & Sons, pgs. 18–30.

Seidel, J., and Kalinowski, M., 2000, ''Pile Set-up in Sands'' Sixth International Conference on the Application of Stress-Wave Theory to Piles: Sao Paulo, Brazil.

Svinkin, M.R. and Skov, R., ''Set-up effect of cohesive soils in pile capacity'', Application of Stress-Wave Theory to piles, 2000: Sao Paulo, Brazil.

Tan, S., Cuthbertson, J, and Kimmerling, R, 2004, ''Prediction of Pile Set-up in Non-cohesive Soils'' Current Practices and Future Trends in Deep Foundations, Geotechnical Special Publication No. 125, DiMggio, J.A., and Hussein, M.H., Eds, American Society of Civil Engineers: Reston, VA.

YPLOT, NOTE03

C: Skin Friction Centroid Factor

Reference A:

Local Practice on OCELL Bi-Directional Test Method

(Extracted from OCELL Test Report Appendix)

Skin Friction Envelop	**Triangular Friction**	**Rock Socketed**	**Short Pile in Rock Socketed**
C Factor	0.67	0.80	0.90~1.00

Document NOTE03, Reference A

Local Practice on OCELL Bi-Directional Test Method

(Extracted from OCELL Test Report Appendix)

CONSTRUCTION OF THE EQUIVALENT TOP-LOADED LOAD-SETTLEMENT CURVE FROM THE RESULTS OF BI-DIRECTIONAL LOAD TEST (BDLT)

Introduction:
BDLT can provide a good estimate of a curve showing the load versus settlement of a top-loaded driven or bored pile (drilled shaft) with the following assumptions, which is consider good sense and usually conservative:

1. The end bearing load-movement curve in a top-loaded shaft has the same loads for a given movement as the net (subtract buoyant weight of pile above hydraulic jack) end bearing load-movement curve developed by the bottom of the hydraulic jack when placed at or near the bottom of the shaft.

2. The side shear load-movement curve in a top-loaded shaft has the same net shear, multiplied by an adjustment factor 'F' for a given downward movement as occurred in the BDLT for that same movement at the top of the jack in the upward direction. The same applies to the upward movement in a top-loaded tension test. Unless noted otherwise, a factor F=0.95 for compression in cohesionless soils and F=0.80 for tension tests in all soils is used.

3. The pile behaves as a rigid body, but includes the elastic compressions that are part of the movement data obtained from a bidirectional load test (BDLT). Procedure 1 interprets an equivalent top-load test (TLT) movement curve and procedure 2 corrects the effects of the additional elastic compressions in a TLT.

4. The part of the shaft below the hydraulic jack (one or multi level) has the same load-movement behavior as when top-loading the entire shaft. The subsequent 'end bearing movement curve' refers to the movement of the entire length of shaft below the jack.

Procedure 1:
Figure A shows BDLT results and Figure B shows the construction of equivalent top loaded settlement curve. Each of the curves shown has points numbered from 1 to 12 such that the same point number on each curve has the same movement magnitude.

With the above assumptions, the equivalent curve can be constructed as follows:
Select an arbitrary movement such as the 0.40 inches to give point 4 on the shaft side shear load movement curve in Figure A and record the load of 2,090 tons in shear at that movement. With the initial assumption of a rigid pile, the top of pile moves downward the same as the bottom. Therefore, find point 4 with 0.40 inches of upward movement on the end bearing load movement curve and record the corresponding load of 1,060 tons.

Adding these two loads will give the total load of 3,150 tons due to side shear plus end bearing at the same movement and thus gives point 4 on the Figure B load settlement curve for an equivalent top-loaded test. Procedure 1 can be used to obtain all the points in Figure B up to the component that moved the least at the end of the test, in this case point 5 in side shear.

Suitable hyperbolic curve fitting technique can be used for extrapolation of the side shear curve to produce end bearing movement data up to 12. Some judgment is required for deciding on the maximum number of data points to provide good fit with high correlation coefficient, r^2. Using the same movement matching procedure described earlier, the equivalent curve to points 6 to 12 can be extended. The dashed line shown in Figure B, signify that this part of the equivalent curve depends partly on extrapolated data.

If the data warrants, the extrapolations of both side shear and end bearing to extend the equivalent curve to a greater movement than the maximum measured (point 12) will be used. An appendix in this report gives the details of the extrapolation(s) used with the present BDLT and shows the fit with the actual data.

<u>Procedure 2</u>:
The elastic compression in the equivalent top load test always exceeds that in the BDLT. It produces more top movement and also additional side shear movement, which then generate more side shear, more compression, etc. An exact solution of this load transfer problem requires knowing the side shear vs. vertical movement (t-y) curves for a large number of pile length increments and solving the resulting set of simultaneous equations or using finite element or finite difference simulations to obtain an approximate solution for these equations.

The attached analysis P.6 gives the equations for the elastic compressions that occur in the BDLT with one or two levels of hydraulic jacks. Analysis P.7 gives the equations for the elastic compressions that occur in the equivalent TLT. Both sets of equations do not include the elastic compression below the hydraulic jack because the same compression takes place in both the BDLT and the TLT. This is equivalent to taking $l_3 = 0$. Subtracting the BDLT from the TLT compression gives the desired additional elastic compression at the top of the TLT. The additional elastic compression is then added to the 'rigid' equivalent curve obtained from Part 1 to obtain the final, corrected equivalent load-settlement curve for the TLT on the same pile as the actual BDLT.

Note that the above p.6 and p.7 give equations for each of three assumed patterns of developed side shear stress along the pile. The pattern shown in the center of the three is applicable to any approximate determined side shear distribution. Experience has shown the initial solution for the additional elastic compression, as described above, gives an adequate and slightly conservative (high) estimate of the additional compression versus more sophisticated load-transfer analyses as described in the first paragraph of this Part II.

The analysis p.8 provides an example of calculated results in English units on a hypothetical 1-stage, single level BDLT using the simplified method in Part II with the centroid of the side shear distribution 44.1% above the base of the hydraulic jack. Figure C compares the corrected with the rigid curve of Figure B. Page 9 contains an example equivalent to that above in SI units.

The final analysis p.10 provides an example of calculated results in English units on a hypothetical 3-stage, multi level BDSLT using the simplified method in Part II with the centroid of the combined upper and middle side shear distribution 44.1% above the base of the bottom hydraulic jack. The individual centroids of the upper and middle side shear distribution lie 39.6% and 57.9% above and below the middle hydraulic jack, respectively. Figure E compares the corrected with the rigid curve. Page II contains an example equivalent to that above in SI units.

<u>Other Tests</u>: The example illustrated in <u>Figure A</u> has the maximum component movement in end bearing. The procedures remain the same if the maximum test movement occurred in side shear. Then we would have extrapolated end bearing to produce the dashed-line part of the reconstructed top-load settlement curve.

The example illustrated also assumes a pile top-loaded in compression. For a pile top-loaded in tension we would, based on Assumptions 2 and 3, use the upward side shear load curve in <u>Figure A</u>, multiplied by the F = 0.80 noted in Assumption 2, for the equivalent top-loaded displacement curve.

<u>Expected Accuracy</u>: There are only five series of tests that provide the data needed to make a direct comparison between actual, full scale, top-loaded pile movement behaviour and the equivalent behaviour obtained from a BDLT by the method described herein. These involved three sites in Japan and one in Singapore, in a variety of soils, with three compression tests on bored piles (drilled shafts), one compression test on a driven pile and one tension test on a bored pile. The largest bored pile had a 1.2 m diameter and a 37 m length. The driven pile had a 1-m increment modular construction and a 9 m length. The largest top loading = 28 MN (3,150 tons).

The following references detail the aforementioned Japanese tests and the results therefore:

Kishida H. et al., 1992, "Pile Loading Tests at Osaka Amenity Park Project", Paper by Mitsubishi Co., also briefly described in Schmertmann (1993, see bibliography). Compares one drilled shaft in tension and another in compression.

Ogura, H. et al., 1995, "Application of Pile Toe Load Test to Cast-in-place Concrete Pile and Precast Pile", special volume 'Tsuchi-to-Kiso' on Pile Loading Test, Japanese Geotechnical Society, Vol. 3, No. 5, Ser. No. 448. Original in Japanese. Translated by M.B. Karkee, GEOTOP Corporation. Compares one drilled shaft and one driven pile, both in compression.

We compared the predicted equivalent and measured top load at three top movements in each of the above four Japanese comparisons. The top movements ranged from ¼ inch (6 mm) to 40 mm, depending on the data available.

The (equiv./meas.) ratios of the top load averaged 1.03 in the 15 comparisons with a coefficient of variation of less than 10%. These available comparisons help support the practical validity of the equivalent top load method described herein.

L.S. Peng, A.M. Koon, R. Page and C. W. Lee report the results of a class-A prediction by others of the TLT curve from a BDLT on a 1.2 m diameter, 37.2 m long bored pile in Singapore, compared to an adjacent pile with the same dimensions actually top-loaded by kentledge. They report about a 4% difference in ultimate capacity and less than 8% difference in settlements over the 1.0 to 1.5 times working load range – comparable to the accuracy noted above. Their paper was published in March 1999 in the Proceedings of the International Conference on Rail Transit, held in Singapore and published by the Association of Consulting Engineers Singapore.

B.H. Fellenius has made several finite element method (FEM) studies of a BDLT in which he adjusted the parameters to produce good load-deflection matches with the BDLT up and down load-deflection curve. He then used the same parameters to predict the TLT deflection curve. We compared the FEM-predicted curve with the equivalent load-deflection predicted by the previously described Part I and II procedures, with the results again comparable to the accuracy noted above. A paper by Fellenius et. al. titled "BDLT and FE Analysis of a 28 m Deep Barrette in Manila, Philippines", awaiting publication in the ASCE Journal of Geotechnical and Environmental Engineering, details one of the comparisons.

Limitations: The engineer using these results should judge the conservatism of the aforementioned assumptions and extrapolation(s) before utilizing the results for design purposes. For example, brittle failure behaviour may produce movement curves with abrupt changes in curvature (not hyperbolic). However, the hyperbolic fit method and the assumptions used usually produce reasonable equivalent top load settlement curves.

Example of the Construction of an Equivalent Top-Loaded Settlement Curve (Figure B) From BDLT Results (Figure A)

Figure A

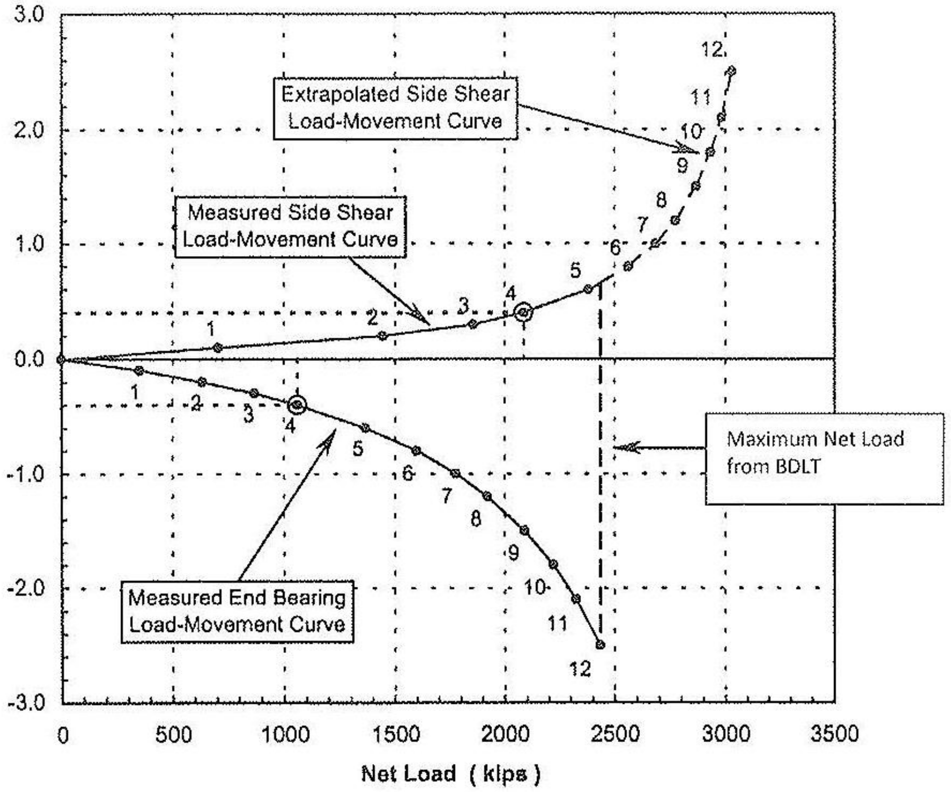

Figure B

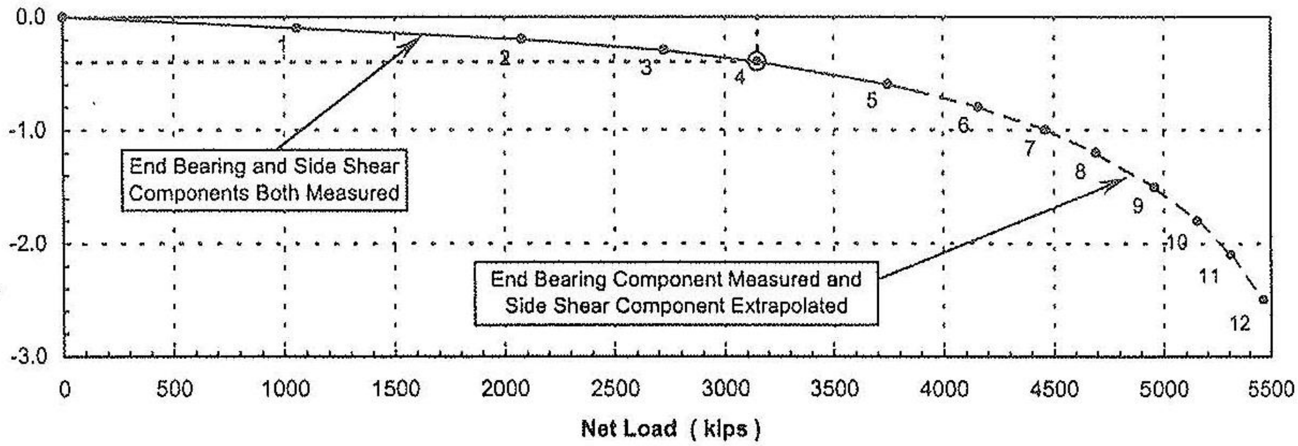

Theoretical Elastic Compression in BDLT
Based on Pattern of Development Side Shear Stress

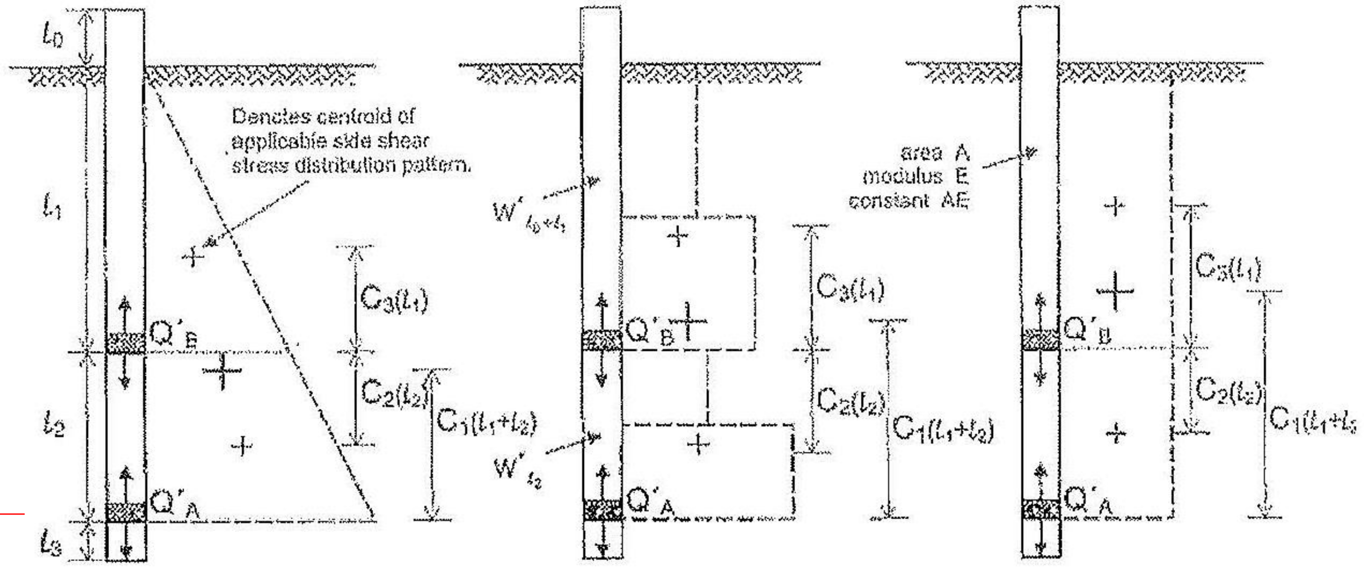

1-Stage Single Level Test (Q'_A only): $\delta_{BDLT} = \delta_{\uparrow e1} + \delta_{\downarrow e2}$

$C_1 = \frac{1}{3}$	Centroid Factor $= C_1$	$C_1 = \frac{1}{2}$
$\delta_{\uparrow(\ell_1+\ell_2)} = \frac{1}{3}\frac{Q'_{\uparrow A}(\ell_1+\ell_2)}{AE}$	$\delta_{\uparrow(\ell_1+\ell_2)} = C_1\frac{Q'_{\uparrow A}(\ell_1+\ell_2)}{AE}$	$\delta_{\uparrow(\ell_1+\ell_2)} = \frac{1}{2}\frac{Q'_{\uparrow A}(\ell_1+\ell_2)}{AE}$

3-Stage Multi Level Test (Q'_A and Q'_B): $\delta_{BDLT} = \delta_{\uparrow e1} + \delta_{\downarrow e2}$

$C_3 = \frac{1}{3}$	Centroid Factor $= C_3$	$C_3 = \frac{1}{2}$
$\delta_{\uparrow\ell_1} = \frac{1}{3}\frac{Q'_{\uparrow B}\ell_1}{AE}$	$\delta_{\uparrow\ell_1} = C_3\frac{Q'_{\uparrow B}\ell_1}{AE}$	$\delta_{\uparrow\ell_1} = \frac{1}{3}\frac{Q'_{\uparrow B}\ell_1}{AE}$
$C_2 = \frac{1}{3}\left(\frac{3\ell_1+2\ell_2}{2\ell_1+\ell_2}\right)$	Centroid Factor $= C_2$	$C_2 = \frac{1}{2}$
$\delta_{\downarrow\ell_2} = \frac{1}{3}\left(\frac{3\ell_1+2\ell_2}{2\ell_1+\ell_2}\right)\frac{Q'_{\downarrow B}\ell_2}{AE}$	$\delta_{\downarrow\ell_2} = C_2\frac{Q'_{\downarrow B}\ell_2}{AE}$	$\delta_{\downarrow\ell_2} = \frac{1}{2}\frac{Q'_{\downarrow B}\ell_2}{AE}$

Net Loads:

$Q'_{\uparrow A} = Q_{\uparrow A} - W'_{\ell_0+\ell_1+\ell_2}$ $\quad Q'_{\uparrow B} = Q_{\uparrow B} - W'_{\ell_0+\ell_1}$ $\quad Q'_{\downarrow B} = Q_{\downarrow B} + W'_{\ell_2}$

W' = pile weight, bouyant where below water table

Q'_B is the 2[nd] level BD-JACK.
For single level YJACK installed, hence ignored Q'_B level.
Only consider Q'_A level.

Theoretical Elastic Compression in Top Loaded Test
Based on Pattern of Development Side Shear Stress

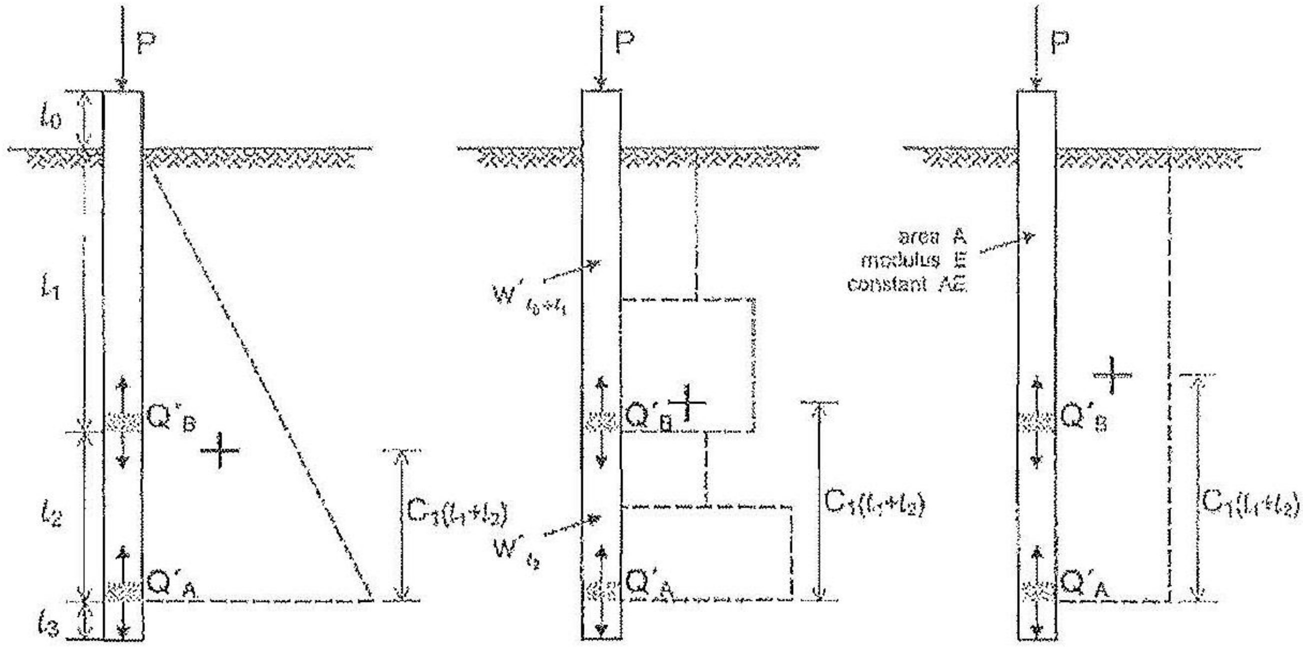

Top Loaded Test: $\delta_{TLT} = \delta_{\downarrow l_0} + \delta_{\downarrow l_1+l_2}$

$\delta_{\downarrow l_0} = \frac{P l_0}{AE}$	$\delta_{\downarrow l_0} = \frac{P l_0}{AE}$	$\delta_{\downarrow l_0} = \frac{P l_0}{AE}$
$C_1 = \frac{1}{3}$	Centroid Factor = C_1	$C_1 = \frac{1}{2}$
$\delta_{\downarrow l_1+l_2} = \frac{(Q'_{\downarrow A}+2P)}{3}\frac{(l_2+l_2)}{AE}$	$\delta_{\downarrow l_1+l_2} = \left[(C_1)Q'_{\downarrow A}+(1-C_1)P\right]\frac{(l_1+l_2)}{AE}$	$\delta_{\downarrow l_1+l_2} = \frac{(Q'_{\downarrow A}+P)}{2}\frac{(l_1+l_2)}{AE}$

Net and Equivalent Loads:

$Q'_{\downarrow A} = Q_{\downarrow A} - W'_{l_0+l_1+l_2}$ $\quad$ $P_{single} = Q'_{\downarrow A} + Q'_{\uparrow A}$ $\quad$ $P_{multi} = Q'_{\downarrow A} + Q'_{\uparrow B} + Q'_{\downarrow B}$

Component loads Q selected at the same (±) Δ_{BDSLT}.

YPLOT, NOTE04

q: Quake Method to compute Residual Settlement

QUAKE Method

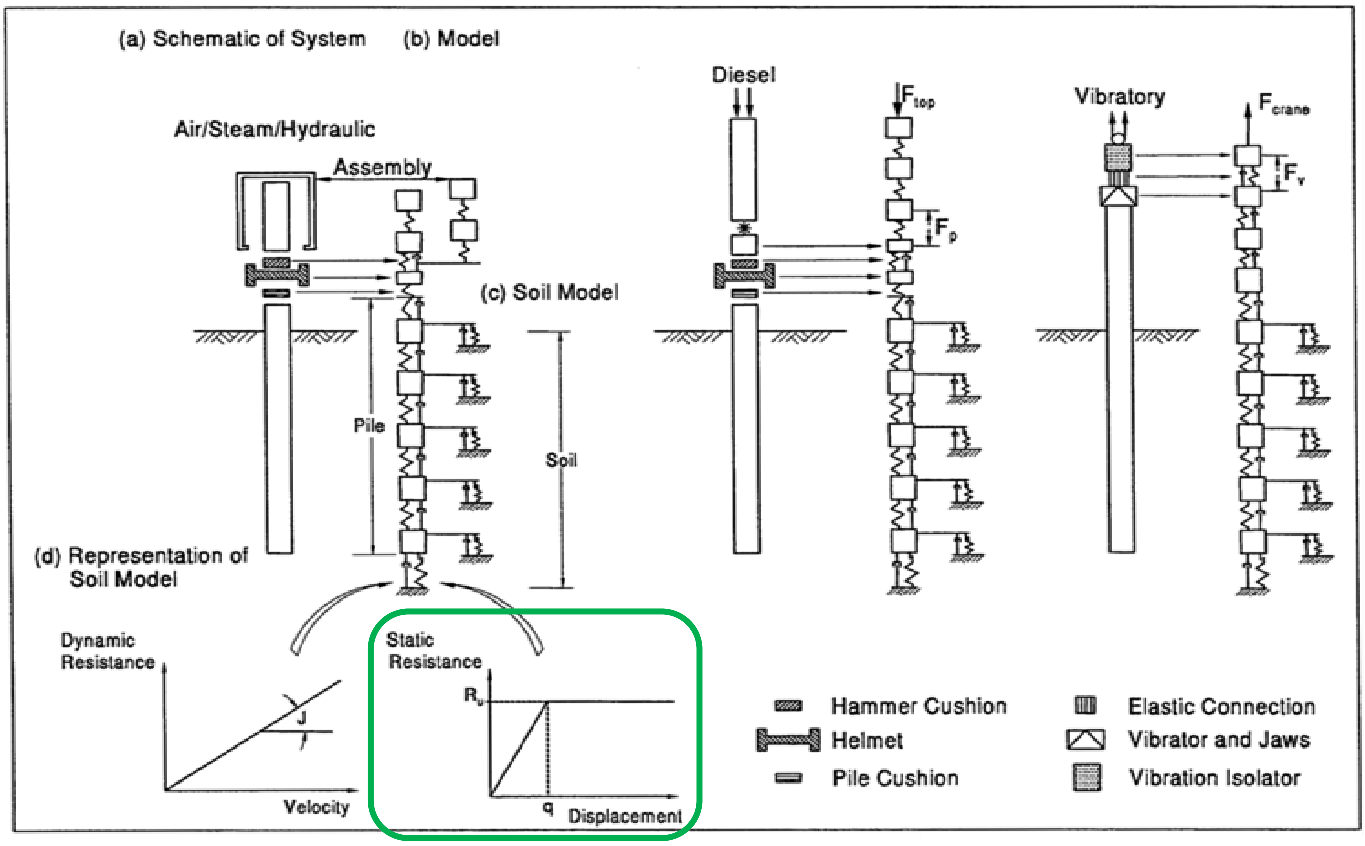

Load-Settlement Behavior in Top-Loaded Kentledge Method vs Bi-Directional YJACK Method

Kentledge Method using MLT Test Procedure	YJACK Method using MLT Test Procedure
s(total) = s(soil) + s(elastic) Q-s Plot obtained by direct measurement method	s(soil) + s(elastic) = s(total) or s(rigid) + s(elastic) = s(total); s(rigid) in SS/CP04 Q-s Plot obtained by s(rigid) from direct measurement combined with s(elastic) from analysis method

The soil static resistance, Rs, will linear increase with pile-soil displacement in the loading stage, until Rs maximum in pile-soil shear occurring from elastic to plastic stage with maximum displacement value q (quake value). This displacement after q-value will form the permanent displacement in the static load~displacement plot.

Quake Method is the pile-soil model in obtaining the residual settlement, s(residual) in YPLOT Analysis; i.e. gap opening after removal of 1X working load (= residual settlement).

Analysis Method	**s(residual)**	**s(@1X working load)**	**s(@2X working load)**
SS/CP4 (2003), Clause 7.6.7	No	Yes	Yes
YPLOT Method	Yes	Yes	Yes

Reference A:

Tech Paper Stress Wave Conference, 1980

(Quake Values determined from Dynamic Measurements)

Reference B:

Research Paper Pile Dynamics, Inc. (PDI), 1980

(Pile Installation Difficulties In Soils with Large Quakes)

Document NOTE04, Reference A

Tech Paper Stress Wave Conference, 1980

(Quake Values determined from Dynamic Measurements)

AUTHIER, J. and FELLENIUS, B. H., 1980. Quake values determined from dynamic measurements. Proceedings 1st International Conference on the Application of Stress-Wave Theory on Piles, Stockholm, 1980. A. A. Balkema, Rotterdam, pp. 197 - 216.

QUAKE VALUES DETERMINED FROM DYNAMIC MEASUREMENTS

JEAN AUTHIER AND BENGT H. FELLENIUS

AUTHIER, J. and FELLENIUS, B. H., 1980. Quake values determined from dynamic measurements. Proceedings 1st International Conference on the Application of Stress-Wave Theory on Piles, Stockholm, 1980. A. A. Balkema, Rotterdam, pp. 197 - 216.

QUAKE VALUES DETERMINED FROM DYNAMIC MEASUREMENTS

JEAN AUTHIER[1)] AND BENGT H. FELLENIUS[2)]

[1)] Terratech Ltd., Montreal, Canada
[2)] University of Ottawa, Canada

In wave equation analysis of pile driving, it is ordinarily assumed that quake values are about 2.5 mm (Smith 1962, Goble and Rausche 1976, Hirsh et al. 1976). Although theoretical studies have been made on the influence of the different parameters used in wave equation analysis, the influence of the quake value has received little attention, only. Forehand and Reese (1964) correlated bearing capacity predictions with results from static loading tests using quake values ranging from 1.3 to 7.6 mm (0.05 in to 0.30 in). The same range of values was used by Ramey and Hudgins (1977) in a study of the sensitivity of the wave equation program solution to the soil parameters used in the analysis. From these studies, it was concluded that the original quake od 2.5 mm value proposed by Smith (1962) is sufficiently precise and that variations of this parameter do not greatly influence the program solution.

In the beginning of the use of wave equation analysis, there was no possibility of determining the quake values for the soils other than by the general correlation of the wave equation analysis with results of loading tests. However, some ten years ago, research at Case Western Reserve University, Cleveland, developed a technique of obtaining measurements of force and acceleration at the pile head during the driving by means of the Pile Driving Analyzer (Goble et al., 1970). The continued development work by the same group resulted in the CAPWAP program (Rausche et al., 1972), which processes the measured dynamic data to determine the soil parameters and the amount of static soil resistance acting on the pile.

In the CAPWAP technique, the computer takes the measured acceleration wave and computes by means of wave equation theory a force curve, which is compared (matched) to the measured force trace. The computation uses mainly six variables — side and toe quake, side and toe damping, and static resistance along the pile shaft and at the pile toe. By changing these variables, the operator strives to achieve agreement (a match) between the computed and measured force traces. The report of the results of the analysis include, amongst others, the ultimate static resistance in the pile and its distribution, the soil quakes, and the soil damping values, as they were assumed in the CAPWAP analysis for the final match.

The CAPWAP technique was used to analyze the results obtained at two different sites showing a large soil quake at the pile toe, as presented in the following.

CASE 1

During a research project on the application of the Pile Driving Analyzer techniques to the Canadian practice, sponsored by the Canadian Government (Fellenius et al., 1978), dynamic data were analyzed from a total of 21 sites across Canada. On one site, closed-toe pipe piles, 324 mm O.D. with wall thicknesses of 7.9 mm, 8.4 mm, and 9.5 mm, were driven into a very dense sandy silty glacial till. Four different hammers were used on the site — one drop hammer and three open-end diesel hammers. The nominal (rated) hammer energies were 27 KJ for the drop hammer and 39 KJ, 46 KJ, and 62 KJ, respectively, for the diesel hammers. Sixteen piles were monitored with the Pile Driving Analyzer.

The average impact stresses for the drop hammer and the diesel hammers were 138 MPa and 117 MPa, 172 MPa and 207 MPa, respectively (20 ksi and 17 ksi, 25 ksi, 30 ksi, respectively). The average transferred energy for the drop hammer was 14 KJ (9 ft-kips). For the diesel hammers, the transferred energies were 11 KJ, 20 KJ, and 41 KJ, respectively (6 ft-kips, 13 ft-kips, 26 ft-kips, ft-kips, respectively). The corresponding energy ratios were 50 % and 28 %, 44 %, and 66 %, respectively. Consistently, the lighter the diesel hammer, the smaller the ratio of transferred energy. Static loading tests showed that the lightest diesel hammer was not able to drive the piles to a sufficient bearing capacity at this site, although this hammer had previously been proven to be adequate for the installation of the same size of piles tp the same desired cpaapcity on other sites in the same general area. During the Analyzer monitoring work, it became evident that the characteristics of the pile-soil system were unusual. This was indicated by the force and velocity wave shapes at termination of driving, which showed an apparent lack of toe resistance at time 2L/c followed by a substantial positive reflected force wave. A representative example of the records is given in Fig. 1. The apparent lack, or, rather, the delay of toe resistance to occur after Time 2L/c resulted in values of bearing capacity calculated by the Analyzer using the Case Method Estimate (CMES), which were considered to be on the conservative side.

In Fig. 2, the results are shown of CAPWAP force matches with, first, the ordinary value of toe quake of 2.5 mm and, then, with a value of 20 mm. A good force match was not possible to achieve with the smaller quake value, only with the larger.

The piling work and CAPWAP analyses took place in June 1976. It was the first time that quake values much larger than the generally assumed value of 2.5 mm were indicated.

CASE 2

Recently, another case was encountered where the Analyzer wave traces indicate a large value of soil quake at the pile toe. Twenty-four 305 mm square precast concrete piles were driven through an about 11 m thick clay deposit and into underlying dense clayey silty glacial till. The pile driving was by means of a Berminghammer B-400 open-end diesel hammer having a rated energy of 62 KJ (40 ft-kips). The pile cushion consisted of layers of plywood.

All piles were monitored with the Pile Driving Analyzer and the dynamic data obtained were similar for all piles.

The driving through the clay was very easy and required a few light blows, only. When the pile toe reached the upper surface of the glacial till at about 11 m depth, the penetration resistance was about 5 blows/0.2 m. Within a penetration of about one metre into the glacial till, the resistance increased to about 40 blows/0.2 m. Then, during the last 150 mm of penetration, the resistance increased from an initial value of 10 blows/cm to a final value of 20 blows/cm. Restriking the pile after one hour gave a resistance of 23 blows/cm. Set-rebound measurements at the end of initial driving, and at restriking, indicated a set of 0.5 mm/blow and a rebound of 15 mm giving a maximum displacement of the pile head of 16 mm. The maximum displacement of the pile toe can be estimated to be about 6 mm by subtracting from the pile head displacement value the calculated value of elastic compression, i.e. 10 mm.

Measurements at two depths have been selected for presentation in this paper; at 11.3 m, when the pile end had penetrated only about 0.3 m into the glacial till and the driving was easy, and at 12.5 m, which is the depth at end-of-driving. The observed dynamic data, including the Analyzer measurements, are compiled in Table 1.

The wave traces, which were recorded at the two depths, are shown in Fig. 3. Both sets of wave traces show the same behavior as observed in Case 1, i.e., a velocity increase at time 2L/c and a delay in the toe-force reflection. In easy driving, upper diagram, the velocity increase is very pronounced, almost indicating a total lack of toe resistance, and the reflection delay is almost two L/c units. At the end of driving, lower diagram, the velocity increase and the reflection delay are less pronounced, but still clearly discernible.

To calculate the pile capacity from the Analyzer measurements by means of CMES directly, a damping value, J, of 0.2 should be applied in this soil. However, as shown in Table 1, this results in capacity values, which are smaller than one normally would be willing to accept as representative of the mobilized pile capacity at the driving. Even the capacity applying J = 0 is considered low considering the penetration resistance and previous experience with the hammer-pile system used.

The reason for the low values is, of course, the reflection delay causing the positive toe reflection to be eliminated from the calculation. It has been proposed that a time delay method be applied to offset the effect of the reflection delay. As indicated in Table 1, the maximum time-delay capacity values are about 30 % higher than the undamped conventional Analyzer capacity. It is probable that a damped time-delay capacity would be about equal to a CAPWAP computed capacity (see below), suggesting that the time delay approach could be used to offset the low conventional values. However, until this is further verified in the field, in cases such as the illustrated Cases 1 and 2, the Analyzer data had better be calibrated by means of a loading test and/or CAPWAP analysis.

CAPWAP analyses were subsequently performed on two representative blow records, one from the depth of 11.3 m and one from 12.5 m. The force matches obtained are given in Figs. 4 and 5 for traces from the depth of 11.3 m and 12.5 m, respectively. For reasons of comparison, the best force match which could be obtained, when applying the conventional quake of 2.5 mm, is given in the upper half of each figure. The matches are quite poor, and the results of the calculations, consequently, or illustrative value, only.

In the lower halves of Figs. 4 and 5, the best matches are shown as obtained with quake values of 20 mm and 8 mm, respectively. The matches, in contrast to those shown for the 2.5 mm quake, are quite good, clearly indicating the necessity of adjusting the computations to the quakes.

It is possible that in the termination driving, depth 12.5 metre, the pile did not mobilize the full static resistance of the soil. The computed maximum pile toe displacement is only about 9mm to 10 mm, which is about equal to or smaller than the quake values of 8 mm and 15 mm assumed in the CAPWAP analysis. A good force match can be achieved with any quake value as large or larger than the displacement value, provided the soil stiffness is kept the same. The mobilized static resistance is then obtained by multiplying the value of the displacement with the value of the soil stiffness. Thus, the CAPWAP analysis results in a minimum quake value equal to the maximum pile toe displacement. The actual quake value of the soil could well be considerably larger.

The foregoing discussion is illustrated in Fig. 6, which shows the force match for a quake of 20 mm. The match is about as good as the match obtained with the 8 mm quake. When the purpose of the CAPWAP analysis is to determine the mobilized static capacity of the pile, the actual quake value used is not important. This should not be understood as if the CAPWAP analysis provides a freedom of quake value to choose. Had the Smith model been built in terms of a certain soil stiffness within the zone of elastic static soil resistance, instead of a quake value, this would have been very clear. As seen in Table 1, the two force matches give the same value of mobilized static soil resistance.

Obviously, when the available hammer energy is not sufficient to mobilize the ultimate soil resistance, as in the present case of refusal driving, neither the Analyzer CMES capacity nor the capacity determined in a CAPWAP analysis can result in anything but the mobilized soil resistance. This capacity can, naturally, be regarded as a least capacity and used as such in the technical design or quality control considerations, as the case may be.

If the capacity is established by means of static loading test, the quake can be determined from the value of ultimate static toe-resistance divided by the soil stiffness value computed in the CAPWAP analysis, provided the driving data analyzed are obtained from restriking the pile at the time of the loading test. In the present case, a loading test for proof testing reasons was performed two days after the driving. The pile withstood a maximum load of 2,800 KN without showing signs of failure. An approximate extrapolation of the load-movement curve suggests a Davisson Limit value of about 3,200 KN. However, the loading test was carried out after the pore pressures induced by the pile driving had dissipated. Therefore, a soil set-up (freeze) must have taken place and the capacity, at the time of the loading test, must in all likelihood have been greater than the static capacity available at the refusal driving. As no restriking was carried out after the loading test, neither the pile-toe quake nor the stiffness of the soil at that time is known. It is probable that both these values changed during the reconsolidation of the soil.

The reason for the unusually large quake observed in the two described cases is not known. The Authors believe it to be related to pore pressure build-up in the soil. However, it is not usually observed at other sites, where similar soils are found. It should also be recognized that the pore pressure dissipation does not always have to result in an appreciable soil set-up.

The occurrence of a large quake has practical importance. Where large quakes occur, a given hammer will not be able to drive a given pile to the capacity possible where the ordinary small quake occurs.

Wave equation analysis with the WEAP program (Goble and Rausche, 1976) is performed for the pile at a depth of 12.5 m using data for the actual hammer and applying the damping factors determined in the CAPWAP analysis. The cushion stiffness was determined to 1,300 MN/m by repeated runs matching the computed values of force, energy and velocity to the Analyzer measured values. Several WEAP runs are made using varying values of pile-end quake. The results are shown in the Bearing Graph in Fig. 7.

The curves in Fig. 7 indicate that when the soil quake increases, the soil stiffness decreases, and, consequently, the maximum capacity to which the hammer can drive the pile reduces. At a site, where the ordinary 2.5 mm quake occurs, the particular hammer-pile-soil combination would be able to achieve a capacity of about 3,000 KN at a practical and economical specified termination resistance of 8 blows/10 mm ("refusal"). As the quake increases, and the soil stiffness decreases, not only does the maximum attainable capacity decrease, the limit of the practical and economical termination criterion reduces, also. In the event of a quake of 15 mm, or rather, a stiffness of about 100 MN/m, not much capacity is gained by driving to a greater resistance than about 3 blows/10 mm.

The Authors believe that large quakes occur more often than one at first would think, but that the soil set-up usually improves the final capacity of the piles so that the inadequate capacity to which the pile has been driven goes undetected. There are, however, many case histories told, where contractors have failed to provide piles with the specified minimum capacity, and where they, subsequently, have been accused of not doing the job properly, and held to add piles, or improve the situation by bringing out larger hammers, etc., to a considerable extra cost to themselves, and/or to the owners. It is quite possible that in many of those cases, the contractor and his original equipment were innocent, and that the blame lies in a large quake without a following soil set-up of appreciable magnitude.

Only the analysis of independent measurements of force and velocity can reveal the existence of a large quake. The presented two case histories provide a sound argument for performing such dynamic measurements.

ACKNOWLEDGEMENTS

The CAPWAP analyses for the two case histories presented were performed by Goble & Associates Inc., Cleveland. Credit for first understanding and showing the existence of the large quake, when discovered in 1976, is due to Dr. Frank Rausche, Cleveland.

The piling contractor for both sites was Bermingham Construction Limited, Hamilton, whose participation and cooperation are gratefully acknowledged.

REFERENCES

FELLENIUS, B. H., SAMSON, L., THOMPSON, D.E., and TROW, W. A., 1978. Dynamic behavior of foundation piles and driving equipment, Terratech Ltd. and The Trow Group Ltd., Department of Supply and Services Research Project, Ottawa, Canada, 520 p.

FOREHAND, P. W., and REESE, J. L., 1964. Prediction of pile capacity by the wave equation, American Society of Civil Engineers, ASCE, Journal of Soil Mechanics and Foundation Engineering, Vol. 90, No. SM2, pp. 1 - 25.

GOBLE, G. G., RAUSCHE, F., and MOSES, F., 1970. Dynamic studies on the bearing capacity of piles, Phase III, Report No. 48, Vol. 1 and Vol. 2, Division of Solid Mechanics, Structural and Mechanical Design, Case Western Reserve University, 325 p.

GOBLE, G. G., and RAUSCHE, F., 1976. Wave equation analysis of pile driving. WEAP program, Vol. 1 - Background, Vol. 2 - User's Manual, Vol. 3 - Program Documentation, US Department of Transportation, FHWA, Office of Research and Development, Washington, 371 p.

HIRSCH, T. J., CARR, L., and LOWERY, L. L., 1976. Pile driving analysis. Wave equation user's manual. TTI program, Vol. 1 - Background, Vol. 2 - Computer Program, Vol. 3 - Program Documentation, US Department of Transportation, FHWA, Office of Research and Development, Washington, 308 p.

RAMEY, G. E., and HUDGINS, A. P., 1977. Sensitivity and accuracy of the pile wave equation", Ground Engineering, Foundation Publishing Ltd., London, Vol. 10, No. 7, pp. 45-47.

RAUSCHE, F., MOSES, F., and GOBLE, G. G., 1972. Soil resistance prediction from pile dynamics, American Society of Civil Engineers, ASCE, Journal of Soil Mechanics and Foundation Engineering, Vol. 98, SM9, pp. 917 - 937.

SMITH, E. A. L., 1960. Pile driving analysis by the wave equation, American Society of Civil Engineers, ASCE, Journal of Soil Mechanics and Foundation Engineering, SM4, Vol. 86, pp. 35 - 61 (Discussions in Vol. 87, SM1, pp. 63-75).

TABLE 1 DYNAMIC DATA FROM CASE 2

	UNIT	DEPTH 11.3 m		DEPTH 12.5 m
DRIVING DATA				
Measured Penetration Resistance	BL/0.2 m	5		400
Measured Net Penetration Per Blow	mm	40		0.5
Measured Rebound Per Blow	mm	15		15
Estimated Maximum Pile Toe Displacement	mm	45		6
ANALYZER DATA				
Peak Impact Force, FIMP	KN	1,600		2,200
Transferred Energy, EMAX	KJ	20		21
CMES Capacity (J = 0.2)	KN	200		1,700
CMES Capacity (J = 0.0)	KN	660		2,200
Maximum Time-Delay Capacity (J = 0.0)	KN	1,000		2,900
CAPWAP DATA				
Assumed Total Capacity	KN	800	2,200	3,200
Assumed Toe Capacity	KN	600	1,900	2,900
Assumed Shaft Capacity	KN	200	300	300
Toe Quake	mm	20	8	15
Shaft Quake	mm	4	2.5	2.5
Soil Stiffness at Toe, K_{soil}	MN/m	30	230	200
Soil Coefficient of Restitution at Toe	- -	1	0.8	0.8
Computed Maximum Toe Displacement, DMAX	mm	30	9	10
Mobilized Total Resistance	KN	600	2,000	2000
Mobilized Toe Resistance	KN	800	2,300	2,300
Case Damping Factor, J_{toe}	- -	0.07	0.22	0.24

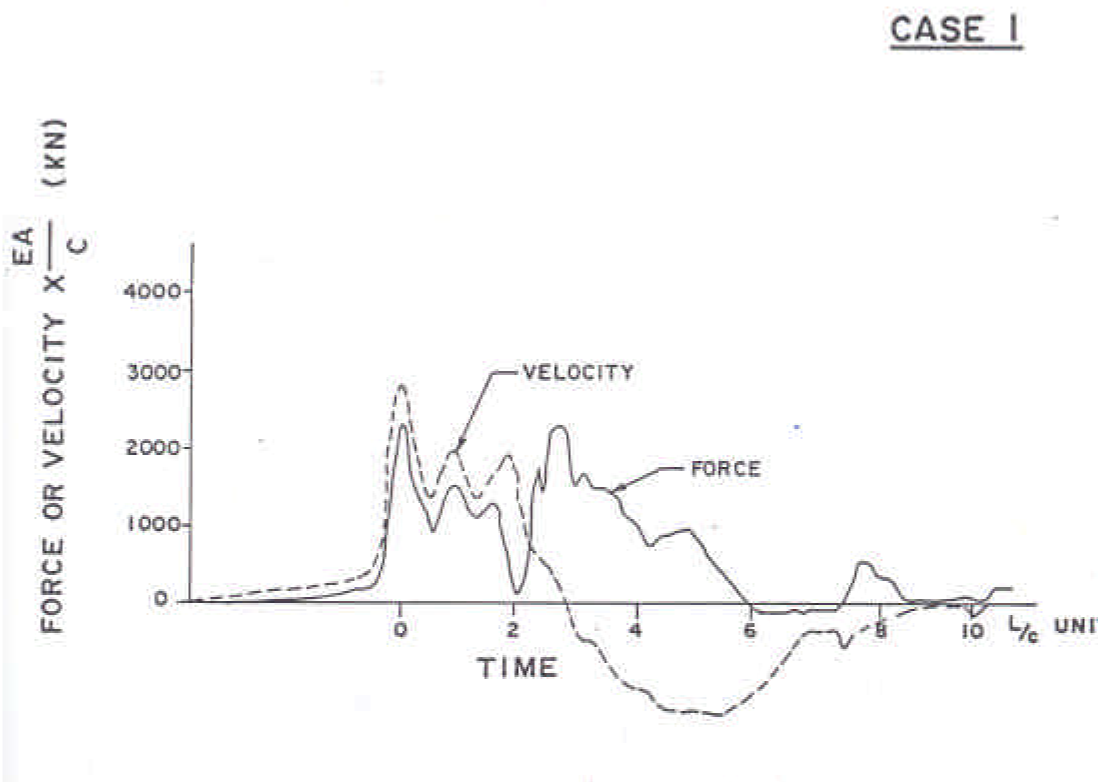

FIG. 1 Force and Velocity Traces, Case 1

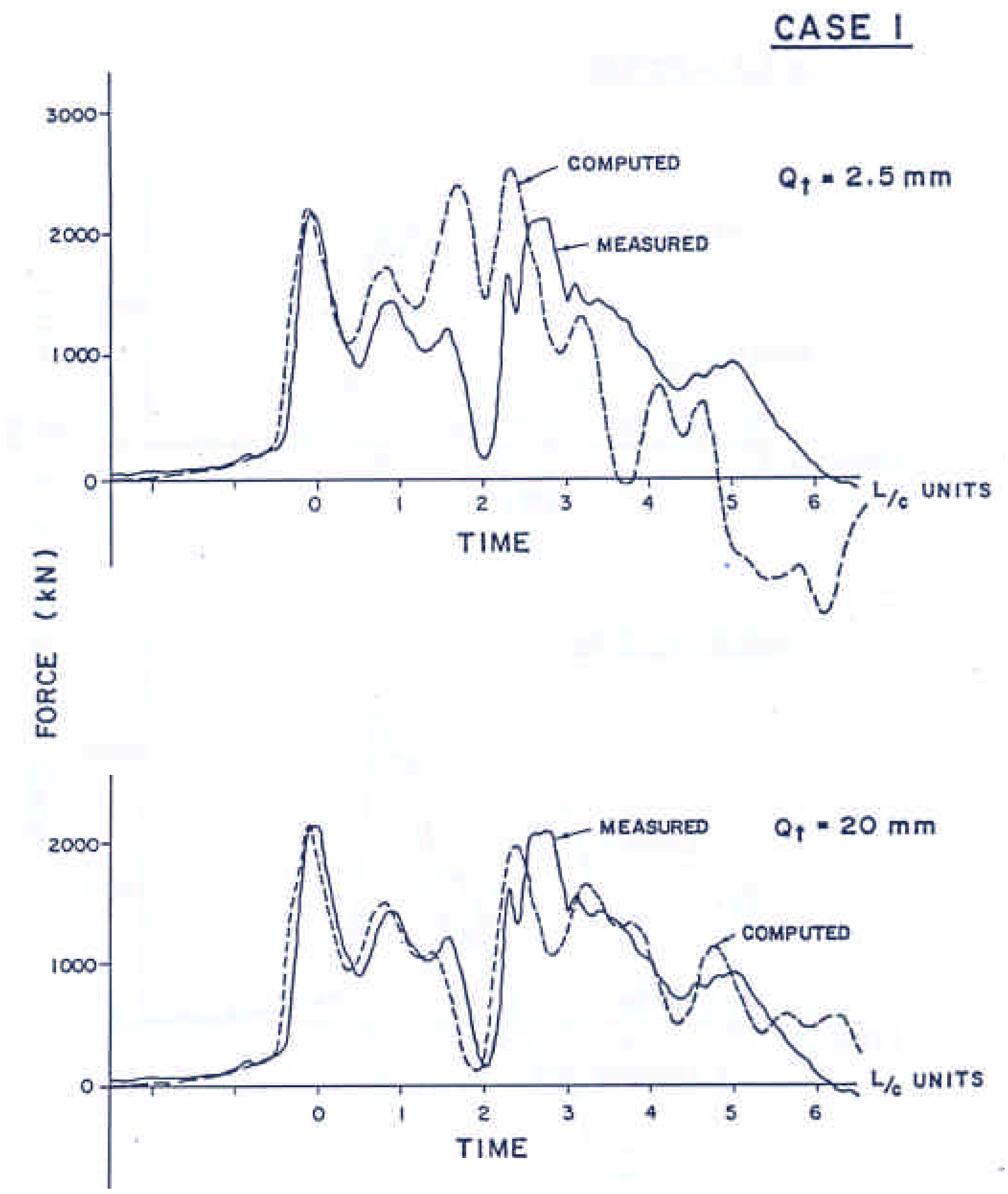

FIG. 2 CAPWAP Force Match for Pile Toe Quake (Q_t) of 2.5 mm and 20 mm, Case 1

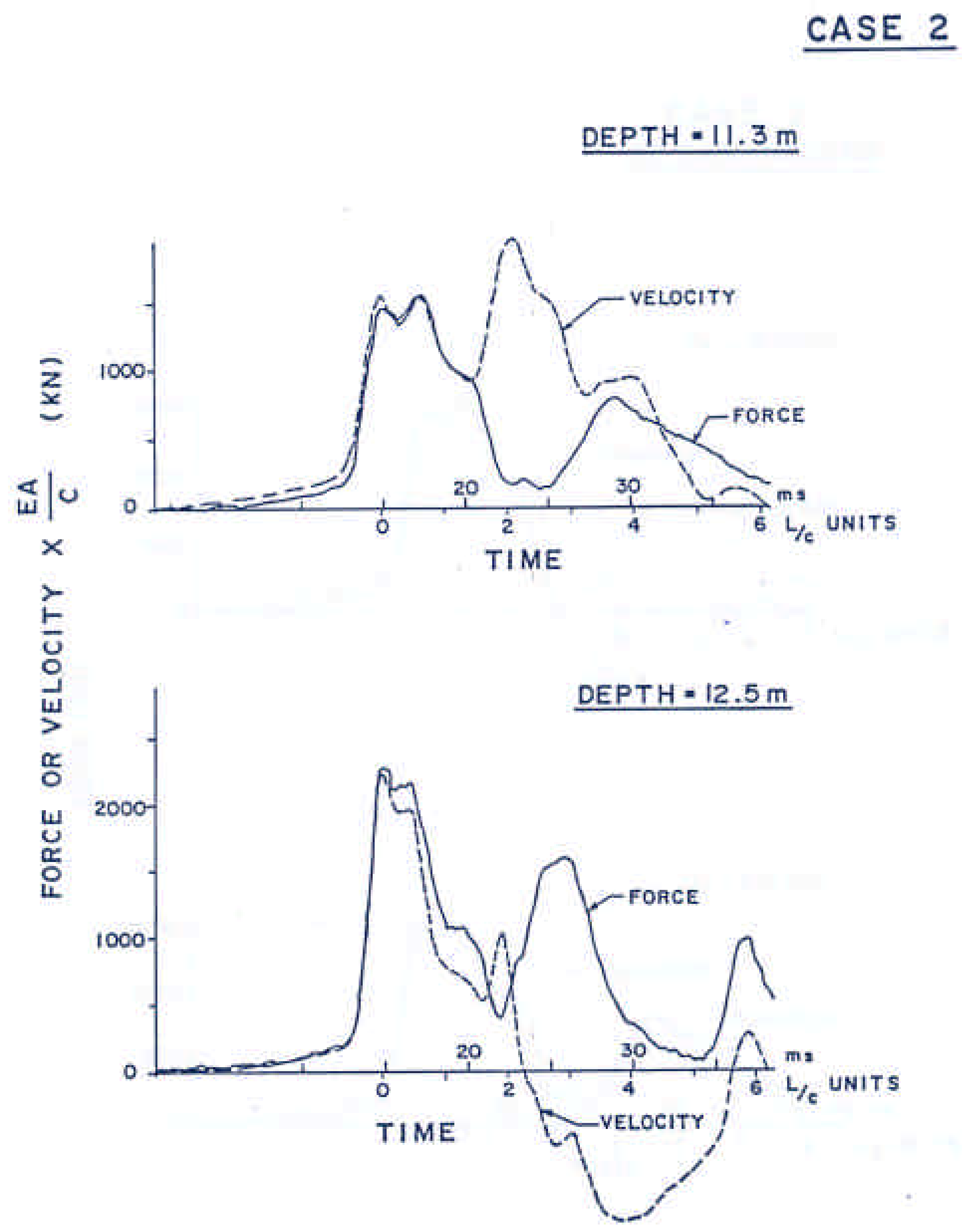

FIG. 3 Force and Velocity Traces at Depths of 11.3 m and 12.5 m, Case 2

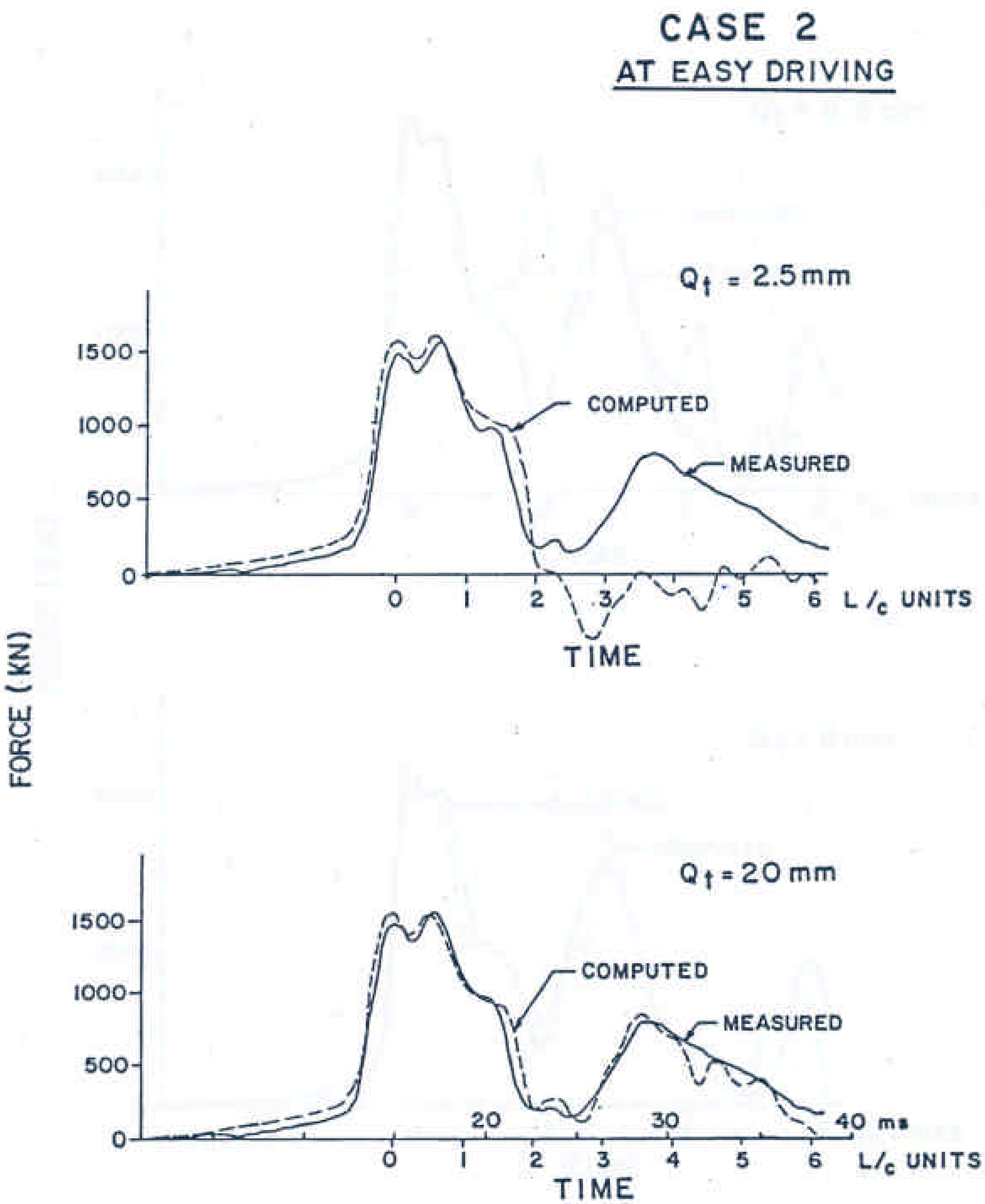

FIG. 4 CAPWAP Force Traces for Pile Toe Quake (Q_t) of 2.5 mm and 20 mm, Depth 11.3 m, Case 2

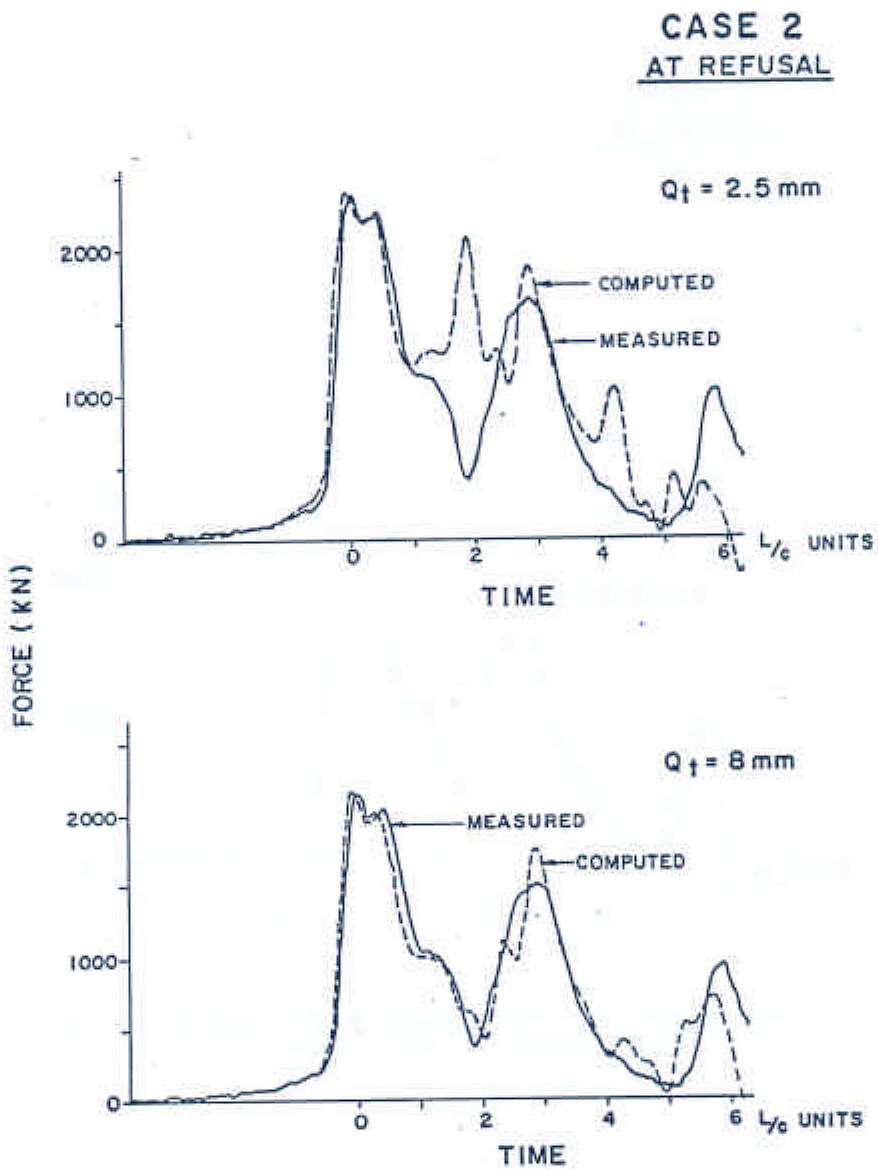

FIG. 5 CAPWAP Force Traces for Pile Toe Quake (Q_t) of 2.5 mm and 20 mm, Depth 12.5 m, Case 2

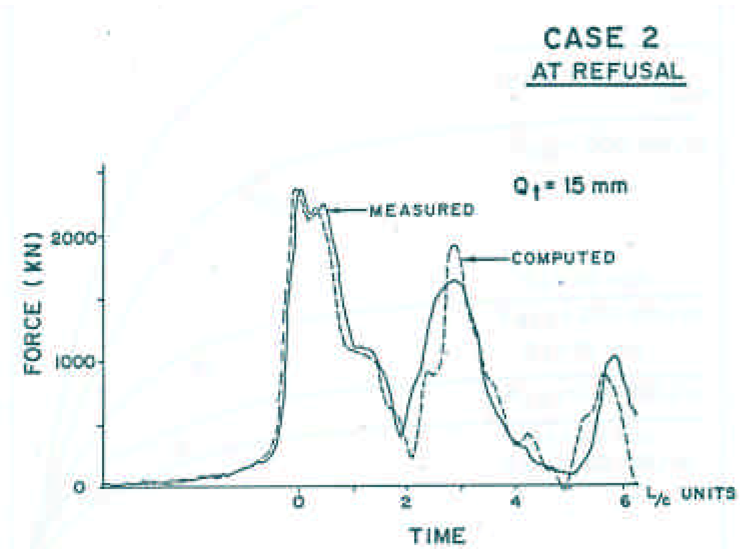

FIG. 6 CAPWAP Force Traces for Pile Toe Quake (Q_t) of 15 mm, Depth 12.5 m, Case 2

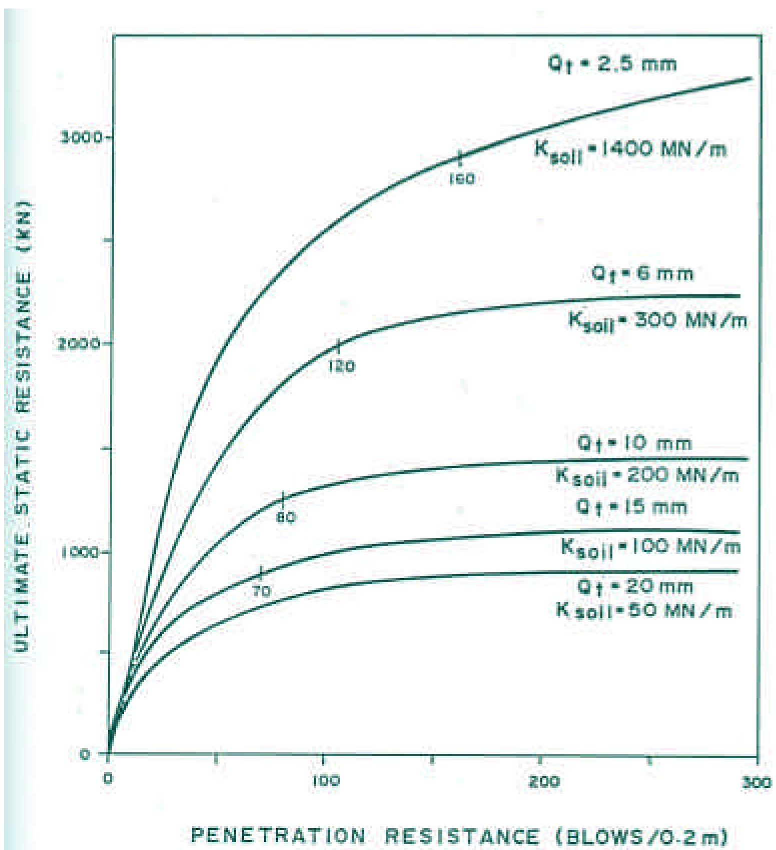

FIG. 7 Bearing Graph from WEAP Analysis with Varying Pile Toe Quake (Q_t) and Soil Stiffness (K_{soil})

Document NOTE04, Reference B

Research Paper Pile Dynamics, Inc. (PDI), 1980

(Pile Installation Difficulties In Soils with Large Quakes)

Pile Installation Difficulties in Soils with Large Quakes

By Garland E. Likins, Jr.*

INTRODUCTION

With the continued development of dynamic pile testing techniques and analysis procedures, much has been learned about the dynamic resistance properties of soils during pile driving. Three types of quantities completely describe the pile during driving; pile forces, pile motions and the soil boundary conditions. If any two are known, then the third can be derived; the CAPWAP computer analysis program (1) utilizes measured force and acceleration data to determine the actual soil parameters. The measured acceleration and Smith type pile and soil models are used to compute a force curve which is then compared with the measured force. Adjustments are made in the soil parameters until the computed and measured force curves match. Output results are then the ultimate static load and its distribution, skin and toe damping values, and skin and toe quakes, i.e., the displacement at which the initial elastic static soil model achieves its ultimate load and goes plastic.

Prior to this analysis technique, it was concluded from parameter studies (2) of the wave equation with the quake between 0.05 and 0.30 inches that the quake value did not significantly affect any of the basic wave equation results. Based on relatively recent experiences using dynamic pile measurement and CAPWAP, it has become apparent that soil quakes far in excess of previously considered values frequently exist and do in fact significantly alter the wave equation results (3,4,5).

This paper discusses three cases where "high quakes" have been observed in soil conditions ranging from sands to clays. Other cases having "high quakes" (toe quakes between 0.4 and 1.0 inches) have also been observed (5). The only apparent common feature in the soils is that they are saturated. In most every case, displacement type piles have been involved and excess pore water pressure buildup during the cyclic pile driving has been suspected. Dissipation of this excess pore pressure usually is accompanied by, but does not necessarily result in, improved soil friction and lower static quakes.

---

*President, Pile Dynamics, Inc., Cleveland, Ohio

EFFECTS OF LARGE QUAKES ON DRIVEABILITY

The occurrence of large toe quakes has complex effects on pile driving which have a great practical importance. First, the ultimate capacity which a hammer attains at refusal driving will be reduced, often requiring the use of a larger hammer. A capacity reduction by a factor of three is easily obtained; as the quake increases, this reduction becomes larger. The reason for this behavior can be observed in Figure 1. For the same maximum toe displacement, a pile with a normal quake will have a much larger permanent set (lower blow count) than will a pile having a large quake. Conversely, to obtain the same blow count, a pile with a large soil quake will require a much larger displacement; thus, more energy is required to mobilize the full resistance for high quake soils. Since the larger energy hammers would not normally be required for the usual soils, refusal blow counts are obtained much earlier, even at low ultimate capacities.

An additional effect of reduced resistance relates to tension reflections. One dimensional wave propagation theory shows that compression impact loads in pile driving cause tension reflections from the pile toe if little soil resistance is present. As soil resistance increases, this tension reflection decreases. If the pile is very short compared to the input pulse length, the continuing input compressive wave superimposed on the upwards traveling reflected tension wave results in little or no net tension. As piles become longer in relation to the input pulse length, net tensions result which can be particularly harmful to concrete piles. In soils with normal quakes, the ultimate load will reach a level approximately 1.2 times the input force at refusal driving and no tension stresses will be present except in easy driving; in the case of piles with medium or long lengths in high quake soils, the ultimate resistance even at refusal driving is much lower than the input force magnitude thus generating these dangerous tension reflections.

These tension reflections are further increased due to the slow response of large soil quakes. With typical pile top cushioning, displacements at the time of arrival of the peak input velocity at every point along the pile are usually comparable in size to normal quakes. Thus, the full resistance effects are mobilized at the time of the first reflection at the pile tip. Under normal conditions, this is enough to prevent damaging tension stresses from occurring. In the large quake case, the displacement at the toe at the arrival of the first input peak (typically 0.1 inch) can be considerably less than the quake. As demonstrated in Figure 1, this of course implies that only a fraction of the toe resistance is initially mobilized (in addition to the ultimate resistance being appreciably reduced) and even higher tension reflections are generated. Only later, after the initial wave peak has been reflected in tension, is the full displacement and resistance achieved. Thus, high tension stresses can be generated even in refusal driving conditions.

The use of dynamic measurements during pile driving has led to real time field evaluation for every blow of capacity, structural integrity, hammer performance and stresses (7). For example, the maximum tension stress T at any location x below the pile top can now be determined from standard Case Method measurements of the force F(t) and velocity v(t) time functions near the pile top from:

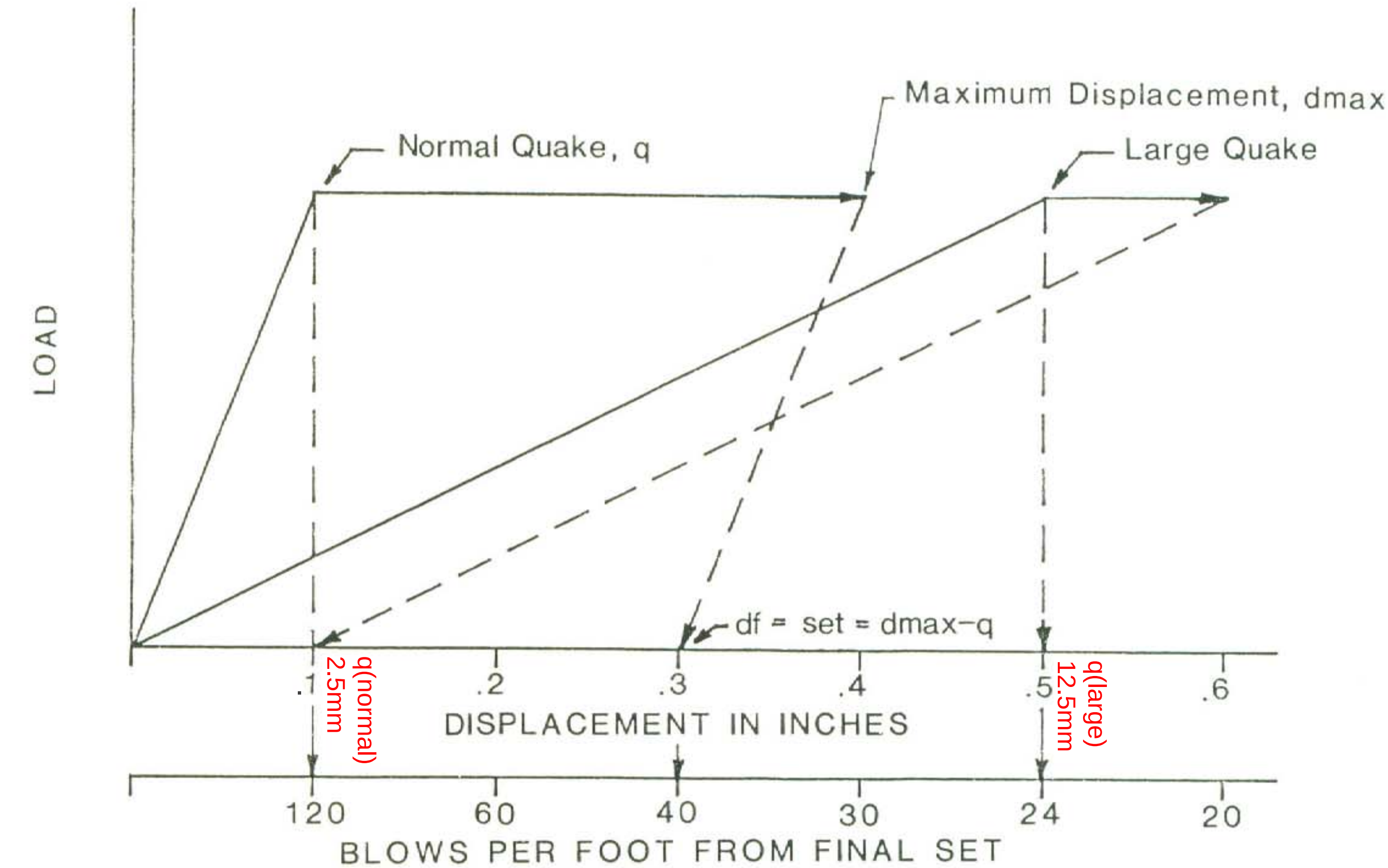

Figure 1: Load Displacement Diagram for Normal and Large Quakes

$$T(x) = \frac{1}{2}\left\{\frac{EA}{C} v\left(\frac{2L}{C}\right) - F\left(\frac{2L}{C}\right) - \frac{EA}{C} v\left(\frac{2L-2x}{C}\right) - F\left(\frac{2L-2x}{C}\right)\right\} \qquad (1)$$

where the times of force and velocity are referenced to the peak input and the E, A, C and L are the pile modulus of elasticity, cross sectional area, speed of stress wave propagation and total length below measuring instrumentation, respectively. The closed form solution for static resistance RS of a one-dimensional travelling wave used in the field analysis equipment is:

$$RS = \left(\frac{1-J}{2}\right)\left\{F(t_1) + \frac{EA}{C} v(t_1)\right\} + \left(\frac{1+J}{2}\right)\left\{F(t_1+\frac{2L}{C}) - \frac{EA}{C} v(t_1+\frac{2L}{C})\right\} \qquad (2)$$

where J is a soil damping constant for soils and time t_1 being the peak input. For large quakes the resistance is low upon the initial arrival of the wave at the pile tip. When time t_1 is delayed from the initial peak, additional toe displacements are introduced into the resistance calculation of Equation 2; these additional displacements will mobilize extra soil resistance and be reflected in the capacity predictions. Investigations of capacity and tension stresses have been made in the field and used to detect the presence of large soil quakes. Although field estimates of quakes can then be made with this information, further laboratory analysis of the data is then usually justified to further define the soil's proper load displacement parameters.

The effects of high input stresses associated with prolonged hard driving, reduced resistance and delayed soil response causing high tension stress from large quakes often then combine to produce unexpected pile damage. Also, the "bounce" or high rebound, often associated with these soil conditions, usually results in a decreased hammer performance. Ram strokes are lower and racking or lift-off of the hammer assembly can become more of a problem due to non-uniform contact stresses and lowering the efficiency of energy transferred into the pile.

CASE STUDIES

Results obtained at three different sites are presented demonstrating the effects of large soil quakes.

Case 1

Several 24-inch (610 mm) octagonal prestressed concrete piles were installed. The piles were hollow, having a cross sectional area of 300 in^2 (1935 cm^2) and were 70 ft (21.3 m) in length. Below 27 ft (8 m), the soil was classified as glacial deposits of hard silty clay. After predrilling the first 12 ft (3.7 m), the pile had been driven to a penetration of 45 ft (13.7 m) with a Kobe K45 open-end diesel hammer which has a rated energy of 91 kip-ft (124 kJ) with a 10-inch (250 mm) plywood cushion and a 3.5-inch (89 mm) Fosterlon capblock. The pile was redriven and tested dynamically after a wait of three days. Blow counts steadily increased to over 21 blows/inch (8 blows/10mm) at 57 ft (17.4 m) penetration. Driving was stopped when the blow count exceeded 50 blows/inch (20 blows/10mm). The cushion was then reduced to only 4 inches (100 mm) of plywood and blow counts decreased to 22 blows/inch (10 blows/10mm) at a ram stroke observed to be 7.7 ft (2.35 m).

Figure 2 shows data taken at the end of driving with the 4-inch (100 mm) cushion. Of special interest is the relative force minimum and velocity maximum at a time 2L/c after the peak input (the time required for the wave to travel the length of the pile, reflect and return to the measuring location which was 60 ft (18.3 m) above the pile toe). Even at refusal blow counts, a net tension of 250 kips (1.1 MN; stress of .83 ksi or 5.75 MPa) is observed at the measuring location 10 ft (3 m) below the pile top. Ordinarily this would indicate a pile with low resistance as compared with the peak force input and structural capacity of the pile. Using techniques previously developed for the calculation of peak tension in the pile from top measurements (6,7), a tension force of 368 kips (1.64 MN) is found 7 ft (2 m) below the transducers. This corresponds to a stress of 1.2 ksi (8.46 MPa). During the actual construction phase of this project, dynamic measurements were again made and indicate that tension stresses as high as 1.5 ksi (10.5 MPa) were present during easy driving.

CAPWAP was used to further investigate the soil response of this pile. Figure 3 shows the final force and velocity matches (Figure 3a uses acceleration as input to compute force, Figure 3b uses force as input to compute velocity) and both are considered good. The total predicted capacity was 500 kips (2.2 MN). The skin friction is distributed rather uniformly with 350 kips (1.6 MN) indicated at the pile tip. However, the indicated toe quake of 0.42 inch (10.7 mm) was equal to the calculated maximum toe displacement, thus accounting for the high blow count. The toe displacement at the arrival time of the first input peak was 0.14 inch (3.6 mm) and therefore mobilized only about half of the total available resistance at the first reflection time. The maximum computed tension force from CAPWAP was 375 kips (1.6 MN). That this tension is high is not surprising considering that the peak force input of 900 kips (4.1 MN, stresses of 3.0 ksi or 21 MPa) is about 1.8 times larger than the bearing capacity during driving.

An equally good CAPWAP match could be obtained with even larger quakes providing the soil stiffness is not changed. It is therefore possible that the toe quake and toe resistance are even larger and the total resistance should be similarly increased. When the hammer in refusal driving is not able to generate sufficient penetration and mobilize the full ultimate soil resistance, dynamic capacity analysis techniques cannot be expected to result in anything greater than the actual mobilized resistance. This, of course, applies equally well to standard wave equation analyses where a driveability limit is obtained or even to static testing when the soil resistance is larger than the jack, reaction capacity or maximum applied proof load; only a lower bound proof load can be determined. A larger hammer would be necessary to achieve additional displacements and mobilize more capacity; however, larger hammers could increase the potential for pile damage.

A second CAPWAP analysis was performed using the same soil constants (resistance distribution and damping factors) except using a standard 0.10 inch (2.5 mm) quake at the pile toe. The toe displacement was equal to the quake at the arrival time of the first input peak at the toe and thus all the available resistance was mobilized. The force and velocity matches shown in Figure 4 are quite poor at 2L/c. The computed

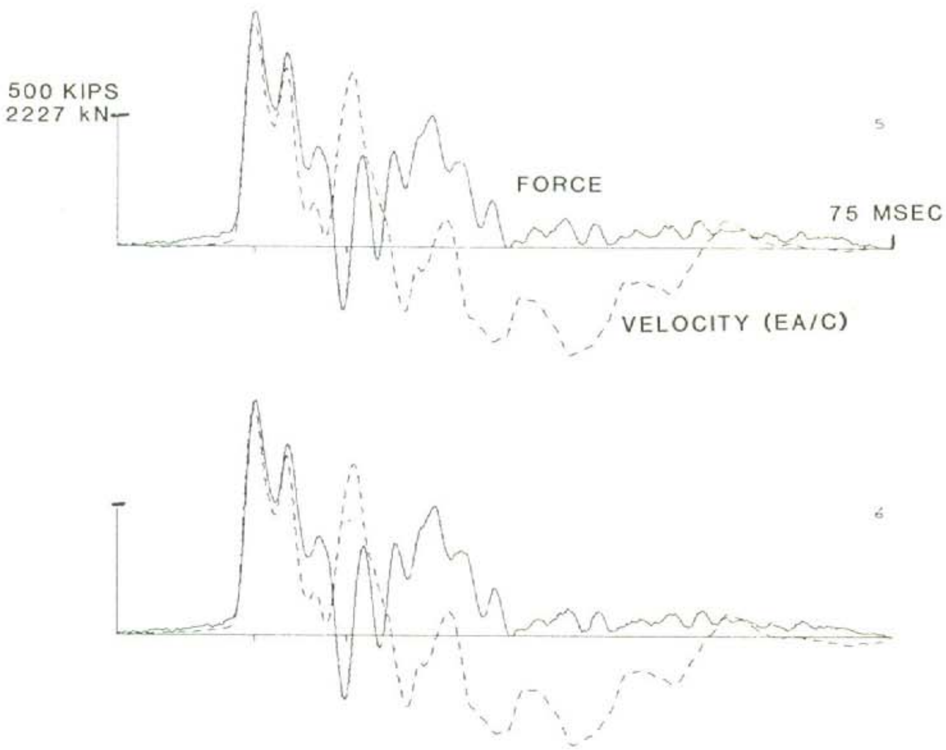

Figure 2: Dynamic Records - Case 1

Case 1

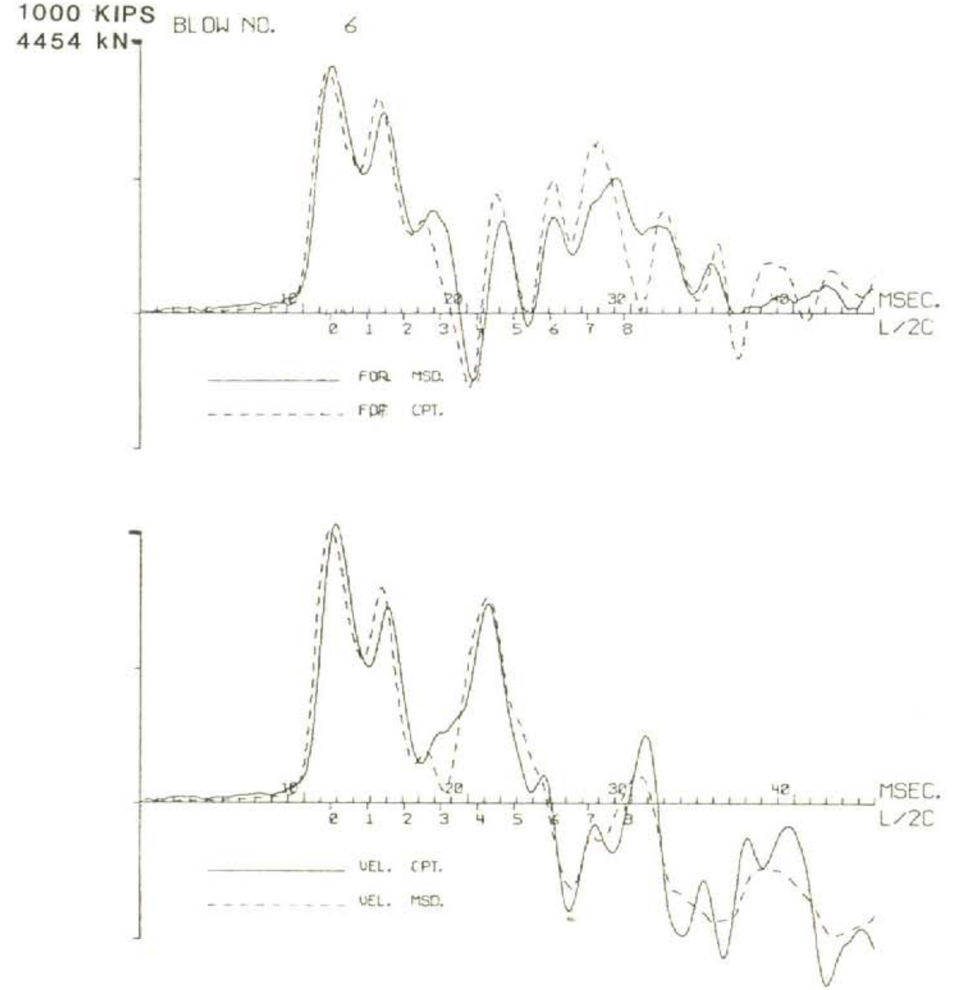

Figure 3: CAPWAP Results with Qt = 0.42 inch

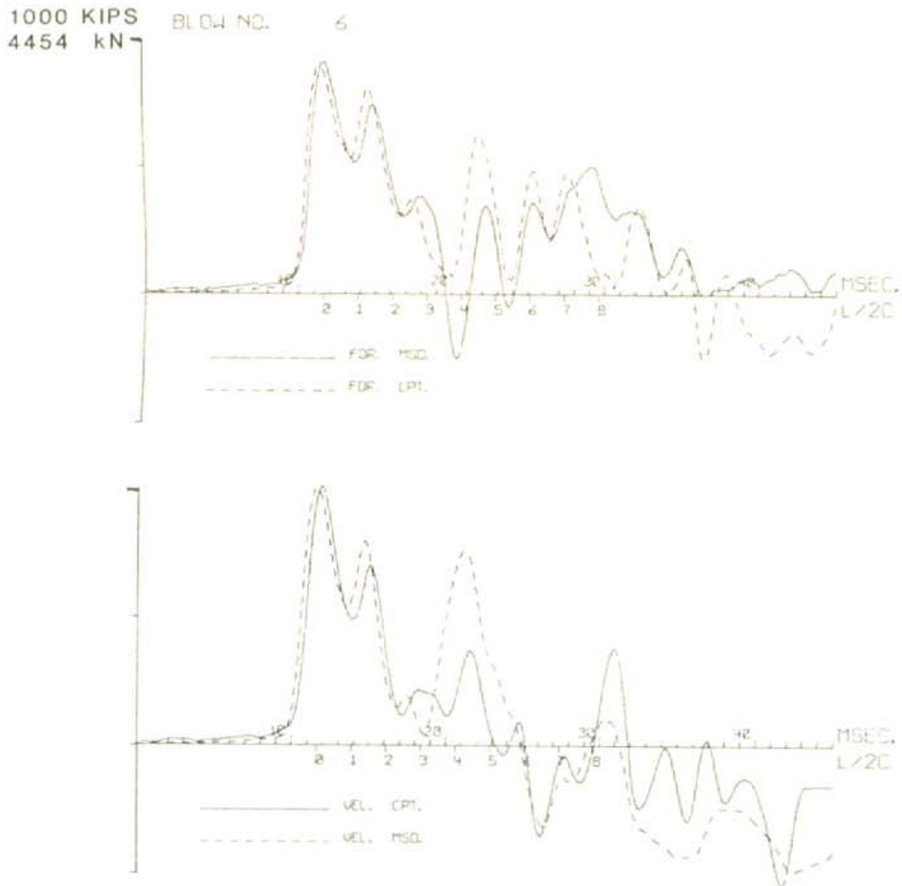

Figure 4: CAPWAP Results with Qt = 0.10 inch

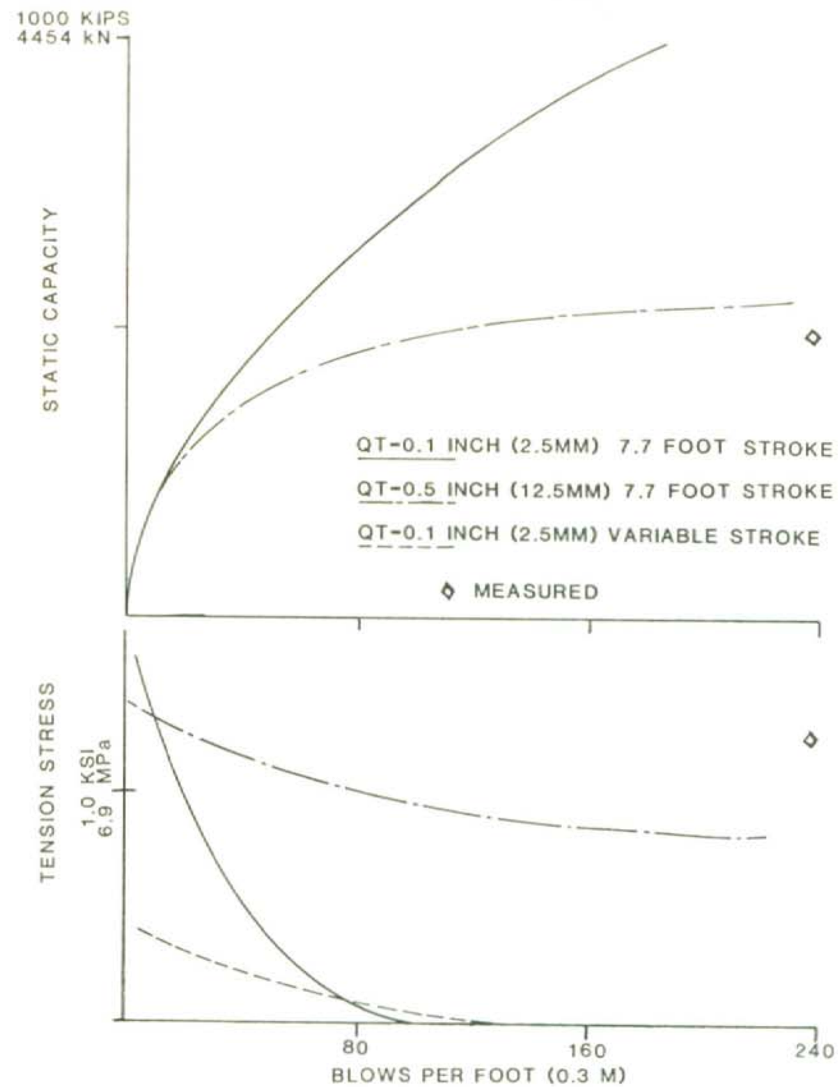

Figure 5: WEAP - Wave Equation Results

force no longer shows a net tension at 2L/c as was actually measured and the computed velocity is significantly reduced. This lack of agreement between measured and computed curves indicate that the soil model with normal quakes is not correct.

The CAPWAP soil model parameters were then input in the WEAP (Wave Equation Analysis Program)(8). Two analysis were made; one with a large quake of 0.50 inch (13 mm) and one with the normal quake of 0.10 inch (2.5 mm). Both analyses used the observed 7.7 ft (2.35 m) stroke. As seen in Figure 5, the capacity using a large quake at 20 blows/inch (8 blows/10mm) is only half the capacity using a small quake. Actually driving beyond 8 blows/inch (3 blows/10mm) yields little increase in capacity. The tension stresses are equally dramatic. Above 6 blows/inch (2 blows/10mm), there is no tension in the pile with normal quakes; with large quakes, the computed tension is never below 0.8 ksi (5.5 MPa) and the measured tension was even higher. The large tension stresses in easy driving may be artificially high as the observed stroke was used throughout. WEAP uses a thermodynamic model for the hammer and if allowed to compute its balanced stroke with a normal quake and 200 kips (890 MN) resistance, a stroke of 5.9 ft (1.8 m) is observed and the maximum tension is then an acceptable 0.3 ksi (2.1 MPa).

This pile was later load tested after several weeks. The Davisson failure load (10) was 1150 kips (5.1 MN). Telltale and strain gage data along the pile length gave excellent correlation with skin friction results from CAPWAP for the first blows at the beginning of this redrive (45 ft or 13.7 m penetration). Equally good results were obtained by comparing restrike capacity information on a 16-inch (405mm) dynamically tested pile driven to approximately 60 ft (18.3 m) penetration and scaling the shaft friction to account for the different diameters, proving the inherent correctness of the dynamic testing techniques (see Figure 6). It is always recommended that at least some piles on each site be tested during restrike to properly assess the soil's static strength. In this manner, setup and relaxation effects are then properly observed.

The large quakes observed dynamically are not in this case reflected in the static load test. It is indeed fortunate that the pore pressure dissipation and soil setup provided additional capacity. Additional testing during production driving, which also included some restrike tests, reconfirmed the indicator pile program results of setup factors of approximately two. Minimum tip elevations resulted in extremely high blow counts for many feet of penetration. A series of blows for one production pile is presented in Figure 7. This prestressed pile had an area of 300 in^2 (1935 cm^2) and a length below transducers of 95 feet (29m). The tension computation of equation 1 shows that tensions of 500 kips (2.3 MN; stresses of 1.7 ksi or 11.5 MPa) are present. Compression forces of 1250 kips (5.7 MN) are much larger than the ultimate capacity of 550 kips (2.5 MN) as determined by CAPWAP (the maximum Case Method estimate from equation 2 with a time search was 540 kips using a damping factor J=0.4 as determined appropriate for this site); the low capacity compared to the peak input is responsible for the high tensions. The CAPWAP analysis showed a toe resistance of 300 kips (1.4 MN). The toe quake was determined to be 0.55 inches (14 mm); this compares with the maximum computed toe displacement of 0.69 inches (17 mm). The driving resistance was in excess of 10 blows/inch (4 blows/10mm). Due to prolonged driving in these high stress conditions, this pile broke suddenly (during blow 6 of Figure 7). The remaining blows of this sequence

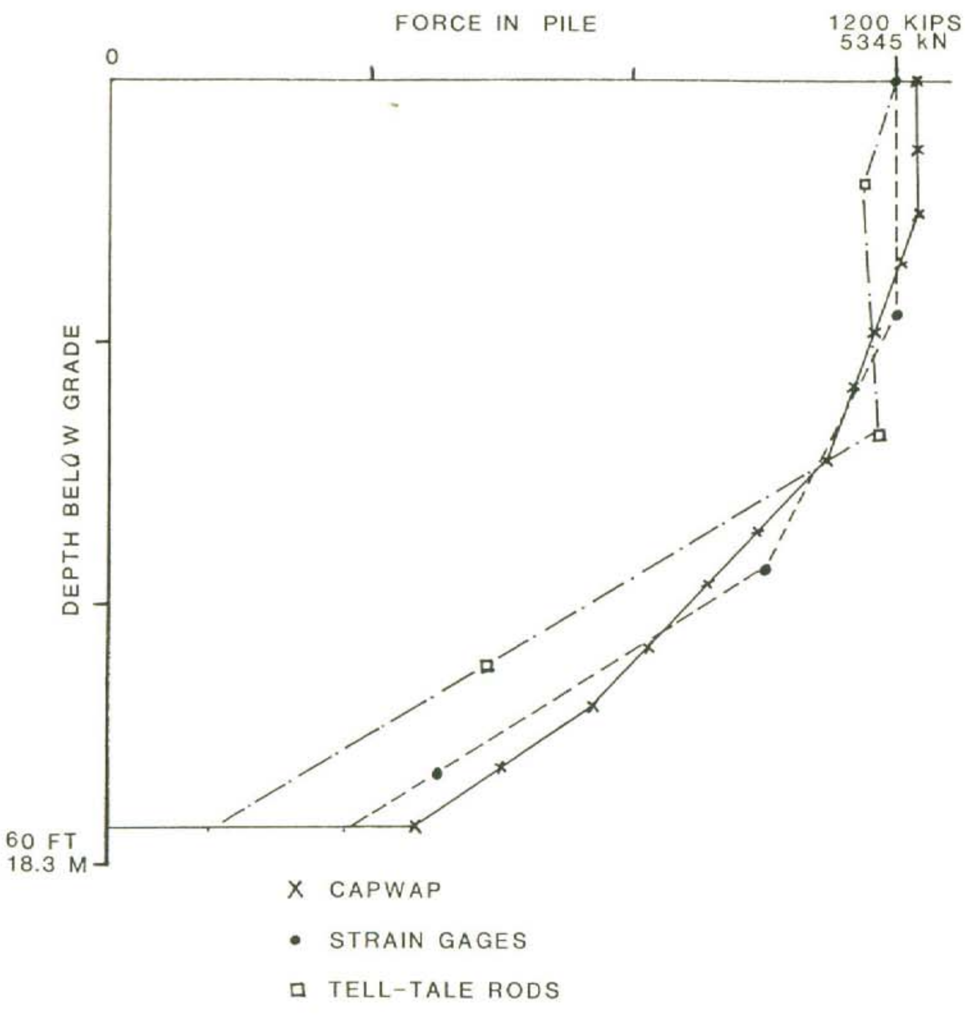

Figure 6: Resistance Distribution

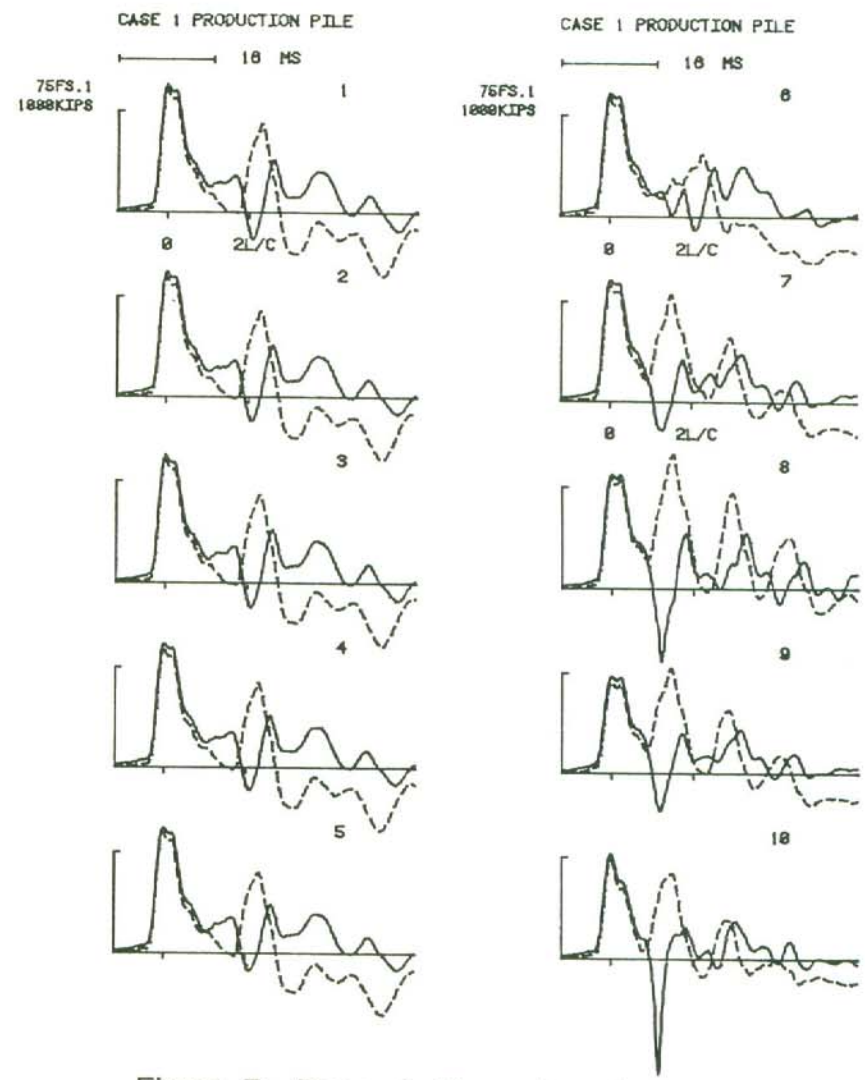

Figure 7: Dynamic Records - Case 1 Production Pile

before the hammer was shut off show a complete break (9) located 56 feet (17m) below the transducers; this is qualitatively observed in the sharp velocity increase and force decrease which is observed before the correct 2L/c time. High tension stresses and some tension cracking were later reduced by preaugering.

Case 2

Seven piles were tested dynamically on this site. All piles were 24-inch (610 mm) square prestressed piles with total lengths below measurements of 122 ft (37.2 m). All were prejetted through gray clayey sand to depths of at least 100 ft (30.5 m) into dense light gray sand. Driving was accomplished by a Raymond 80 hammer with a rated energy of 80 kip-ft (109 kJ).

The dynamic data of two piles is shown in Figure 8. Again, a velocity increase is observed followed by negative (upward or rebound) velocities. In both cases, the blow counts were slightly in excess of 17 blows/inch (7 blows/10mm) and skin friction was minimal. Proportionality between force and velocity for almost the entire first 2L/c indicates no reflections from soil skin resistance or pile cross sectional changes. Observed quakes from CAPWAP were about 0.7 inch (18 mm). Although capacities were around 1000 kips (4454 kN or about 60 percent of the peak force input) in each case, the slow soil response associated with the large quakes produced tension stresses of 0.75 and 1.00 ksi (5.2 and 6.9 MPa) for Piles A and B, respectively. Tension stresses in other piles on this site reached maxima of 1.37 ksi (9.5 MPa) at 4 blows/inch (2 blows/10mm).

No trend in setup or relaxation was observed (verified by restrike testing) on this site as might be expected in a soil described as dense sand.

Case 3

Twelve 18-inch (457 mm) square prestressed piles were driven and tested dynamically using a Delmag D-30 hammer. The pile lengths were 80 ft (24.4 m) and the soil was described as a saturated dense fine sand with some silt or clay content. Again, the piles were prejetted.

Blow counts were erratic at the end of driving ranging from 2 to over 42 blows/inch (1 to 17 blows/10mm). The example case shown in Figure 9 had 17 blows/inch (7 blows/10mm). The maximum computed tension was 0.6 ksi (4.1 MPa) at the end of driving and as large as 1.3 ksi (9.0 MPa) at lower blow counts. Again indicated capacities are low (compared to the peak force input and structural pile strength) as seen by the large velocity increase at 2L/c.

A CAPWAP analysis was not performed on this pile, although analyses of other piles on this site indicated quakes on the order of 0.40 to 0.50 inch (10 to 13 mm).

The analysis of the force and velocity traces revealed that one third of the piles had excessive structural damage (9) below grade, a condition not previously recognized due to the erratic blow counts during driving. It is probable that this damage was caused by the excessive tension due to the large quakes.

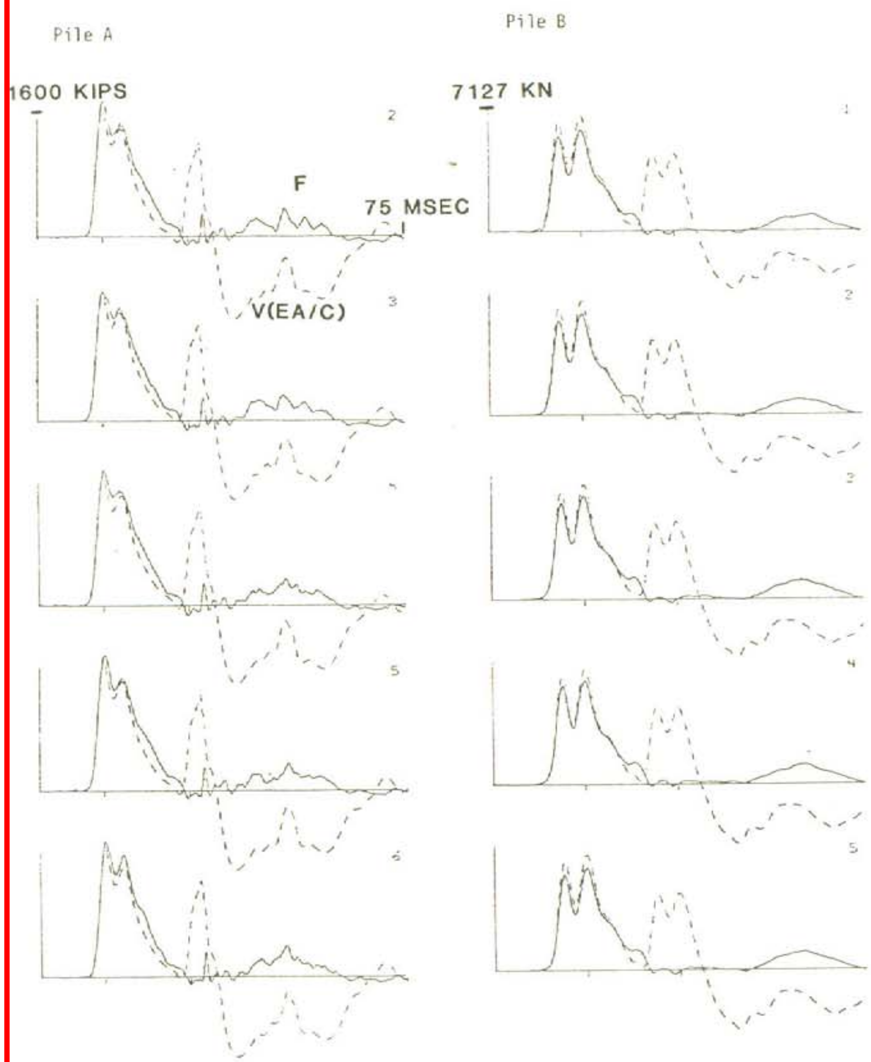

Figure 8: Dynamic Records - Case 2

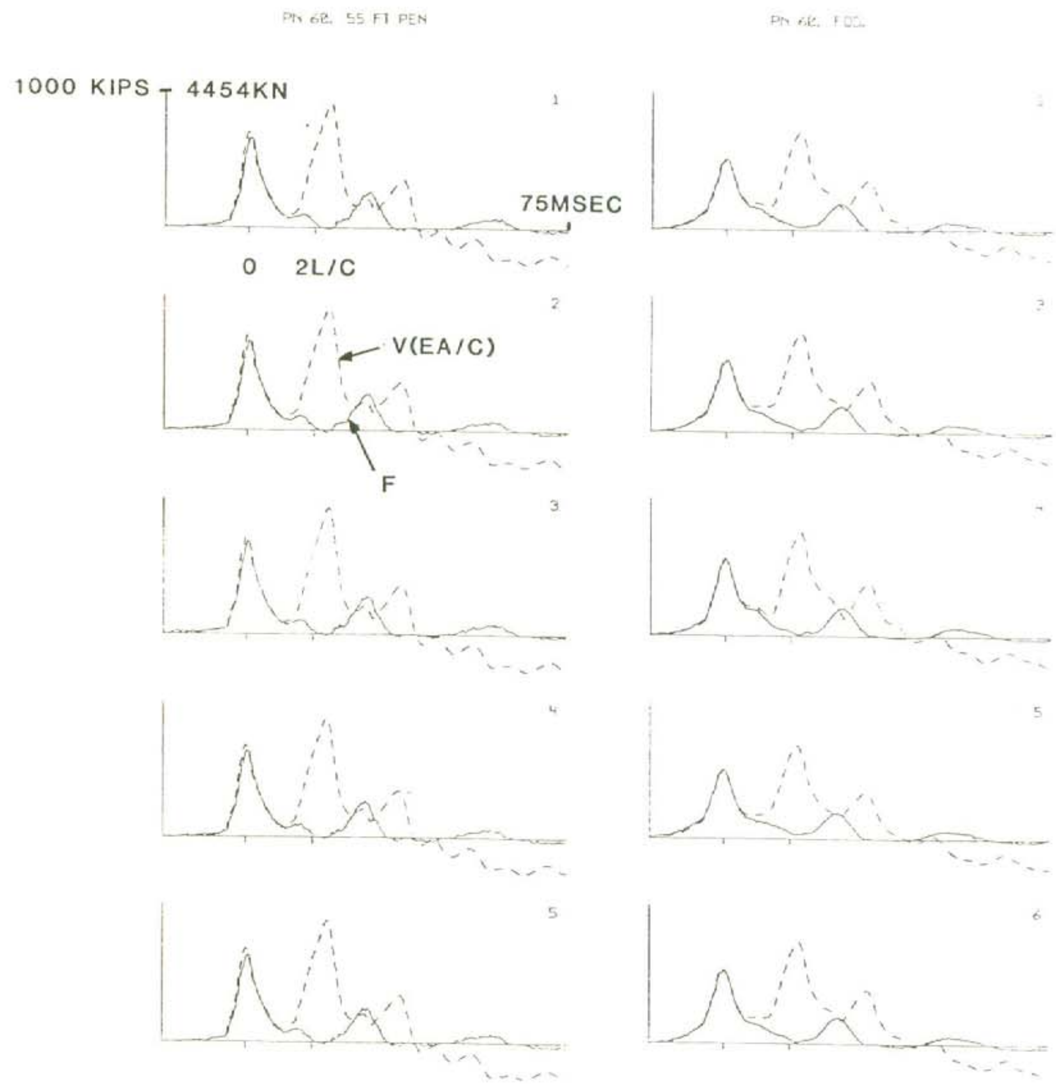

Figure 9: Dynamic Records - Case 3

Large setup factors associated with the fine grained soil and cementation in some layers later provided adequate capacity as determined by restrike testing. However these strength gains were primarily located below the structural damage. These damaged piles would not have been able to support even the design load and detrimental settlements would have resulted.

CONCLUSIONS

The three cases presented here clearly demonstrate the adverse effects of large toe quakes on pile driving. Not only is the driveability and ultimate soil resistance reduced but also increased tension stresses even in refusal driving conditions can and do cause structural damage.

The only common soil condition is saturation. It is felt that excess pore water pressures, caused by displacement piles driven into poorly drained soils is the primary cause of these large quakes.

Reliance only on dynamic formula or wave equation driving criteria could lead to unsafe foundations although in many cases gains in soil strength, as pore pressures decrease, compensate for low initial capacities. The only reliable method of determining the actual soil response during driving is by measurements of force and velocity. Subsequent CAPWAP analysis or low Case Method capacity (when compared with the peak input force) in near refusal conditions can be used to detect this behavior. Restrike testing by Case or CAPWAP Methods should always be performed, especially on sites with saturated or fine grained soils, to confirm service load capacity.

If large quakes are found, several corrective actions may be necessary. Augering with slightly undersize bits through weak layers and even through the problem soils may often be beneficial. Non-displacement pile types could be considered. If concrete piles are long and tension stresses high, the ram weight may be increased and the ram stroke may be reduced, causing lower compressive input and subsequent reflected tension stresses. Pile cushion thickness may be increased resulting in a longer input pulse width and reduced compression and tension wave peaks.

REFERENCES

1. Goble, G.G., Rausche, F. and Moses, F., "Dynamic Studies on the Bearing Capacity of Piles, Phase III", Report No. 48, Division of Solid Mechanics, Structures and Mechanical Design, Case Western Reserve University, 1970, Cleveland.

2. Forehand, P.W. and Reese, J.L., "Prediction of Pile Capacity by the Wave Equation", ASCE J. SMFE, Vol. 90, No. SM2, 1964, pp. 1-25.

3. Authier, J. and Fellenius, B.H., "Quake Values Determined from Dynamic Measurements", Proceedings, Seminar on the Application of Stress-Wave Theory on Piles, Stockholm, Sweden, June 1980.

4. Thompson, C.D., "Discussion on Quake Values Determined from Dynamic Measurements", Proceeding, Seminar on the Application of Stress-Wave Theory on Piles, Stockholm, Sweden, June 1980.

5. Numerous reports on consulting projects by Goble & Associates, Inc., Cleveland, Ohio.

6. Likins, G.E., "Maximum Tension Envelope for a Pile from Case Method Measurements", Presentation at Dynamic Testing of Piles Seminar, Cleveland, Ohio, February 1979.

7. Goble, G.G., Rausche, F. and Likins, G.E., The Analysis of Pile Driving - A State-of-the-Art", Proceedings, Seminar on the Application of Stress-Wave Theory on Piles, Stockholm, Sweden, June 1980.

8. Goble, G.G. and Rausche, F., "Wave Equation Analysis of Pile Driving - WEAP Program", prepared for the U.S. Department of Transportation, Federal Highway Administration, Implementation Division, Office of Research and Development, July 1976.

9. Rausche, F. and Goble, G.G., "Determination of Pile Damage by Top Measurements", Behavior of Deep Foundations, ASTM, STP 670, Raymond Lundgren, Editor, American Society for Testing and Materials, 1979, pp. 500-506.

10. Davisson, M.T., "Pile Load Capacity", Proceedings, Design, Construction and Performance of Deep Foundation, ASCE - University of California, Berkley, August 1975.